AD

USAAVLABS TECHNICAL REPORT 66-9

FATIGUE CRACK PROPAGATION IN AIRCRAFT MATERIALS

By

William G. Degnan
Peter D. Dripchak
Charles J. Matusovich

March 1966

U. S. ARMY AVIATION MATERIEL LABORATORIES
FORT EUSTIS, VIRGINIA

CONTRACT DA 44-177-AMC-84(T)
SIKORSKY AIRCRAFT
DIVISION OF UNITED AIRCRAFT CORPORATION
STRATFORD, CONNECTICUT

Disclaimers

The findings in this report are not to be construed as an official Department of the Army position unless so designated by other authorized documents.

When Government drawings, specifications, or other data are used for any purpose other than in connection with a definitely related Government procurement operation, the United States Government thereby incurs no responsibility nor any obligation whatsoever; and the fact that the Government may have formulated, furnished, or in any way supplied the said drawings, specifications, or other data is not to be regarded by implication or otherwise as in any manner licensing the holder or any other person or corporation, or conveying any rights or permission, to manufacture, use, or sell any patented invention that may in any way be related thereto.

Trade names cited in this report do not constitute an official endorsement or approval of the use of such commercial hardware or software.

Disposition Instructions

Destroy this report when no longer needed. Do not return it to the originator.

DEPARTMENT OF THE ARMY
U. S. ARMY AVIATION MATERIEL LABORATORIES
FORT EUSTIS, VIRGINIA 23604

This program was performed under Contract DA 44-177-AMC-84(T) with Sikorsky Aircraft Division of United Aircraft Corporation.

The data contained in this report are the result of research conducted to determine the fatigue crack propagation of aircraft materials. Fatigue crack propagation tests as well as fracture toughness and tensile tests have been conducted on various aircraft materials, including steel, aluminum, titanium, magnesium, and glass reinforced plastics.

The report has been reviewed by the U.S. Army Aviation Materiel Laboratories and is considered to be technically sound. It is published for the exchange of information and the stimulation of future research.

Task 1P1215901A14227
Contract DA 44-177-AMC-84(T)
USAAVLABS Technical Report 66-9
March 1966

FATIGUE CRACK PROPAGATION IN AIRCRAFT MATERIALS

Sikorsky Engineering Report Number SER-50411

By

William G. Degnan
Peter D. Dripchak
Charles J. Matusovich

Prepared by

Sikorsky Aircraft Division of United Aircraft Corporation
Stratford, Connecticut

for

U. S. ARMY AVIATION MATERIEL LABORATORIES
FORT EUSTIS, VIRGINIA

ABSTRACT

The influence of metallurgical, chemical, and geometric variables on fatigue crack propagation rates was investigated in alloys of aluminum, magnesium, steel, and titanium. Some limited fatigue crack propagation was done in laminated plastics. A possible correlation between fatigue crack propagation, fracture toughness, and tensile strength was also investigated.

All materials have been ranked according to their resistance to fatigue crack propagation. The critical plane strain fracture toughness (K_{Ic}), critical plane stress fracture toughness (K_c) (where applicable), ultimate tensile strength, and per cent elongation were also reported for all materials.

For the materials tested in this program, there was no appreciable thickness or chemical effect. Shot-peening did increase resistance to fatigue crack propagation. In general, there was an increase in the resistance to fatigue crack propagation in materials with greater ductility. The correlation between fatigue crack propagation and static fracture toughness was very poor. The crack propagation results of laminated plastics was also considered unsatisfactory.

Further research is needed to determine the effect of steady and vibratory stresses on fatigue crack propagation. Research is needed to determine the relationship between fatigue crack propagation and fracture toughness parameters.

PREFACE

This report is submitted in accordance with United States Army Aviation Materiel Laboratories Contract Number DA 44-177-AMC-84(T), Investigation of Fatigue Crack Propagation in Aircraft Materials. Research was conducted from February 25, 1963 to August 31, 1965 in the contractor's test facilities located at:

Sikorsky Aircraft Division of United Aircraft Corporation
Main Street, Stratford, Connecticut

The following personnel were directly associated with this research program:

Administrative Task Coordinator - Horace W. Bonnett
Technical Task Coordinator - William G. Degnan
Test Engineer - Peter D. Dripchak
Test Engineer - Charles J. Matusovich

Authors of this report were:

William G. Degnan
Peter D. Dripchak
Charles J. Matusovich

BLANK PAGE

CONTENTS

ILLUSTRATIONS

TABLES

SYMBOLS

E	modulus of elasticity in tension
e	elongation (tensile) in a two-inch gage length
π	constant, equal to 3.141
μ	Poisson's ratio, unit lateral contraction divided by unit longitudinal elongation
F_{ty}	0.2% offset tensile yield strength
F_{tu}	ultimate tensile strength
psi	pounds per square inch
ksi	thousands of pounds per square inch
2a	fatigue crack length (natural fatigue crack in fatigue crack propagation but includes length of machined slot in fracture toughness specimens)(see Figures 1 and 10)
2b, w	width of specimen
K	stress intensity factor (psi$\sqrt{\text{inch}}$) of elastic stress field in the vicinity of the crack tip
G	energy to propagate a crack (inch-pounds per inch) or strain-energy release rate as the crack extends
K_{Ic}	critical stress intensity factor associated with initiation of unstable plane-strain fracturing (stress intensity factor needed to start a crack propagating under a static load)
K_c	critical stress intensity factor associated with initiation of unstable plane-stress fracture (stress intensity factor needed to produce an unstable crack under a static load)
G_{Ic}	critical crack extension force associated with initiation of unstable plane-strain fracturing

G_c	critical crack extension force associated with initiation of unstable plane-stress fracturing
σ_g	gross stress across uncracked cross-sectional area of fatigue crack propagation or fracture toughness specimens
Δ	difference between successive readings (as in $\Delta(2a)/\Delta N$, crack propagation rate)
α	evaluated geometric correction factor (crack length versus finite specimen width)
v	vertical displacement of two points (one inch above and one inch below a crack under static load) as measured with a compliance gage

INTRODUCTION

Fatigue research on a systematic basis has been conducted since the first published works of Wöhler in 1860. Although many attempts have been made to develop a basic theory of the mechanism of fatigue, most researches have resulted chiefly in an accumulation of observations of the associated phenomena. For the present study, a logical division of fatigue crack initiation and crack propagation has been followed. Fail-safe design concepts require an intimate knowledge of crack propagation, or "cracked life".

A wide range of rotorcraft inspection intervals and methods exists. Intervals may range from one-half hour to one thousand hours; methods may range from a cockpit display to a full tear-down inspection. While past service experience remains an excellent guide to the choice of methods and intervals of inspection, knowledge of fatigue crack propagation mechanics serves as a method of comparison for the substitution of a new material for an old and as a design technique in making decisions in new design applications.

Recent researchers have shown a correlation between a material's notch toughness and its fatigue propagation rate. This research program was designed to explore this notch toughness relationship further, with the main aims:

1. To rank materials for their resistance to fatigue crack propagation.

2. To obtain a statistically reliable basis of test information on which to base further testing and comparisons.

3. To obtain corollary information from other mechanical testing (fracture toughness and tensiie tests).

In this project, the stress intensity factor

$$K = \alpha \sigma_g \sqrt{a}$$

$$\text{where } \alpha = \frac{\sqrt{4 + 2\ (a/b)^4}}{2 - (a/b)^2 - (a/b)^4}$$

$$\text{if } a < b$$

as originally proposed by Greenspan, Reference 5, was used for the data reduction.

EXPERIMENTAL PROCEDURE

Fatigue Crack Propagation Test Procedure

The specimen used in these tests is shown in Figure 1. The specimen was precracked by flexing over a sharp corner or between a pair of pre-loaded knife edges with an electric motor-driven Krouse eccentric head, Figure 2. The length of the pre-crack was controlled to approximately 1/2 inch by cementing small copper wires to the specimen at the desired crack end point. The wires were connected to an electrical relay that stopped the machine when the wire broke. This is known as the "micro-wire" or "fail wire" technique.

Fatigue crack propagation tests were conducted on both Wiedemann-Baldwin IV-4F and IVY Company IVY-12 constant-load fatigue machines equipped with 5:1 load amplifiers, Figures 3 and 4. All load measurements were made using a calibrated load cell in series with the specimen under test. In both the load cell calibration and the specimen test setup, an Ellis BA-12 bridge amplifier and a cathode-ray oscilloscope were used to measure the output of the load cell. The overall limit of error of this entire system of measurement is estimated, conservatively, as five percent.

Early research indicated that the greatest difficulty in measurement of crack length was the determination of the vanishingly small apex of the fatigue crack. This problem was solved through the use of birefringent plastic and circularly polarized light at an incident angle to the specimen of forty-five degrees. A specific interference pattern is found in the back-reflected light locating the apex of the fatigue crack with considerable accuracy and repeatability. (Suitable plastics, adhesives, and related accessory items are available commercially as "Photostress" from the Budd Company, Instruments Division, Phoenixville, Pa.) Figure 5 is a photograph of a fatigue crack propagation specimen taken from one of the film strips made during this research program.

In tests of plastic laminate specimens, shear failures of the adhesive used to bond the birefringent plastic to the specimen precluded the use of this method of locating the apex of the fatigue crack. In these cases, direct measurement of the crack length was made using the plastic laminate's characteristic opaque line in the vicinity of the crack.

Crack lengths were recorded by time lapse photography. The photographic exposure rate was controlled by a timer at 1 frame each 10 seconds or 1 frame each 30 seconds. In addition, a series switch actuated by the rotating unbalanced mass of the fatigue testing

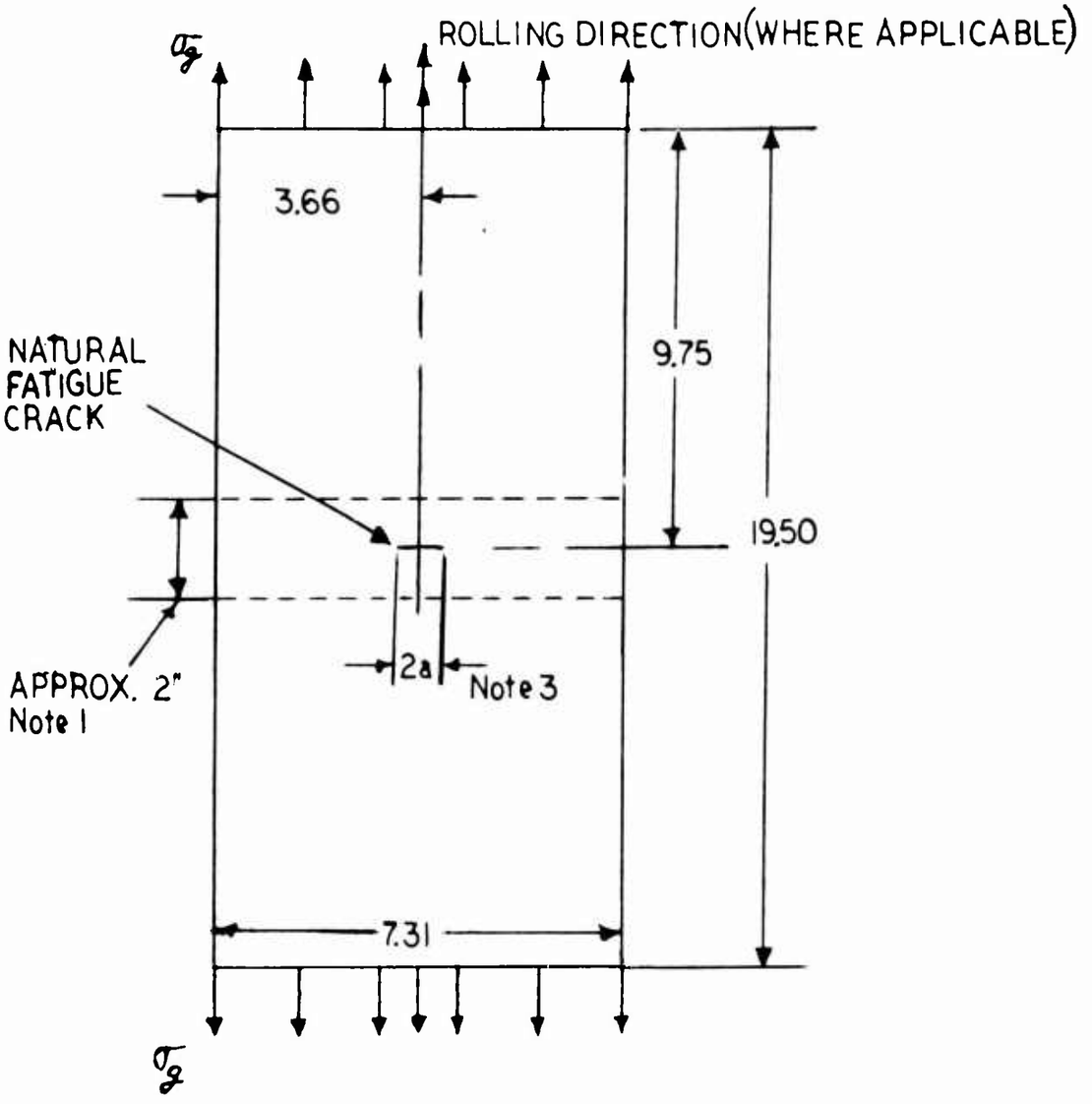

Note 1: Birefringent Plastic Bonded to this Area
Note 2: Five-Hole Bolt Pattern Drilled (Both Ends) for Fatigue Machine Fittings.
Note 3: Length of Initial Crack (2a) Ranged from 1/2 to 1 Inch

Figure 1. Fatigue Crack Propagation Specimen

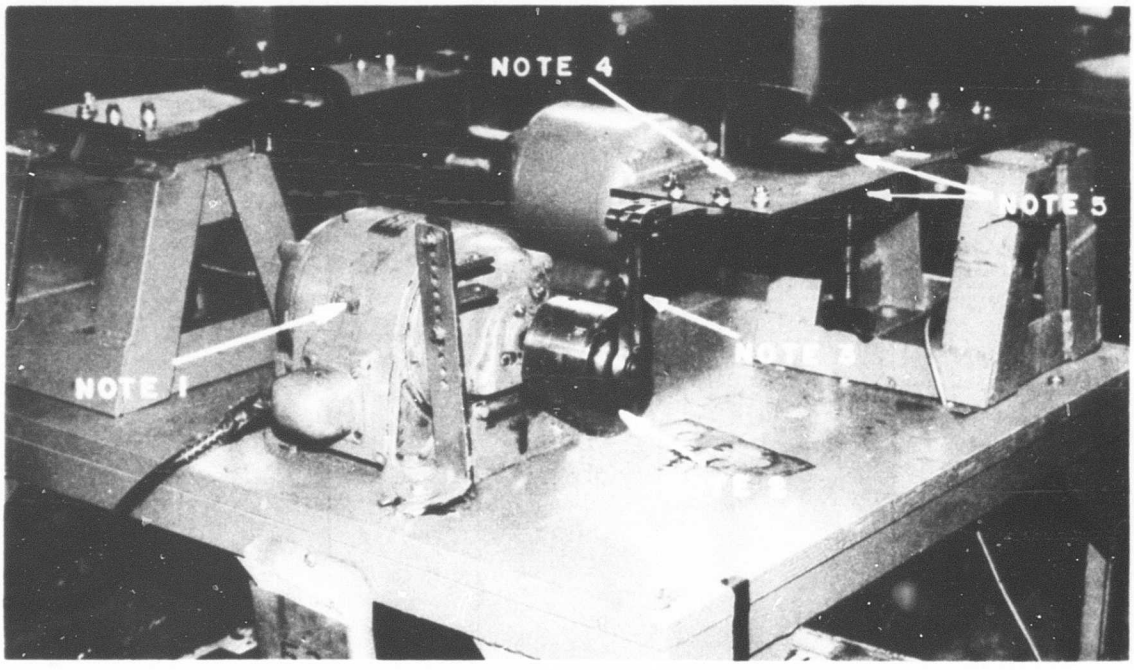

Note 1: 1½-Horsepower AC Motor
Note 2: Eccentric Head
Note 3: Connecting Crank
Note 4: Fatigue Crack Propagation Specimen
Note 5: Knife Edges and Supports
Note 6: Micro-wire not Visible in this Photograph

Figure 2. Natural Fatigue Crack Flexure Machines

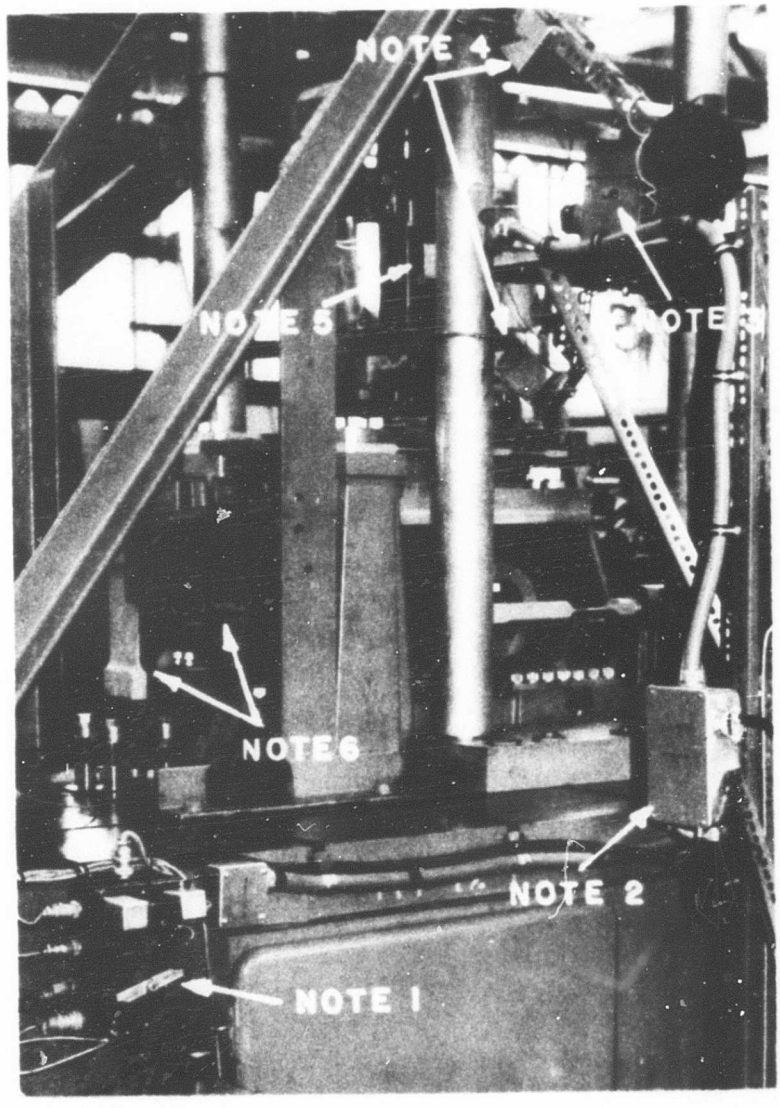

Note 1: Elapsed-Time Photographic Control Box
Note 2: Part of the Monitoring System (See Figure 6)
Note 3: 35 MM Single Frame Advance Camera
Note 4: Upper and Lower Strobe Lights
Note 5: Portion of the Fatigue Crack Propagation Specimen (See Figure 4)
Note 6: 5:1 Load Amplifier

Figure 3. Fatigue Crack Propagation Test Setup on the IVY-12

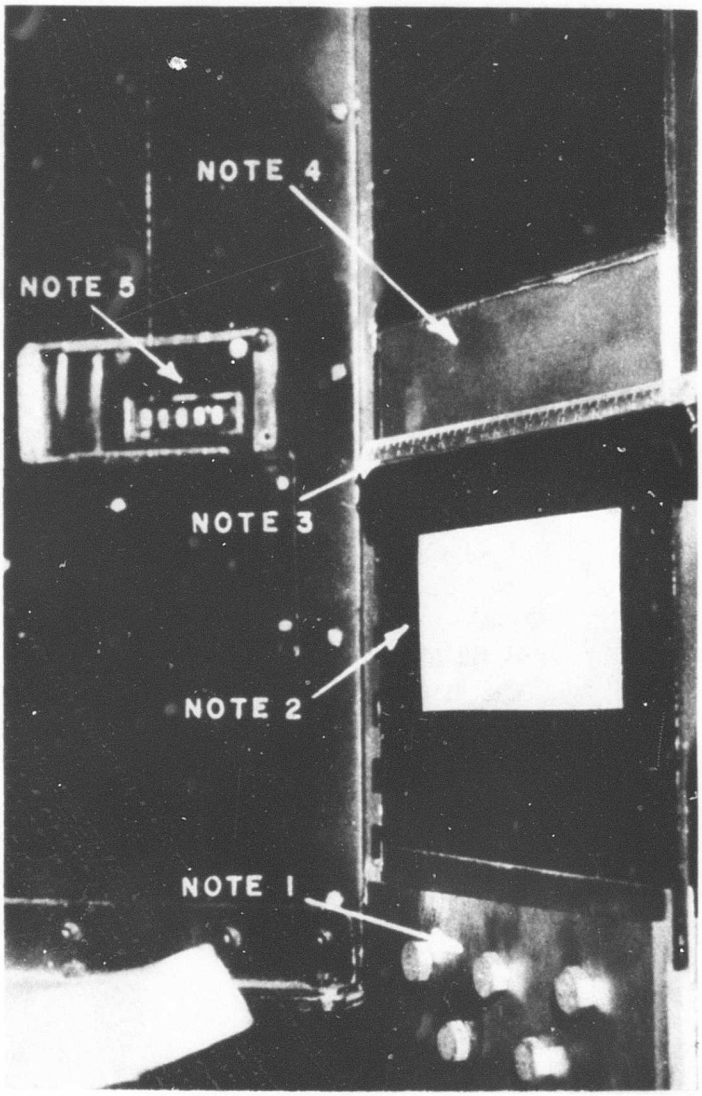

Note 1: Fatigue Machine Fitting, Showing the Five-Hole Bolt Pattern
Note 2: Identification Card Attached to the Specimen
Note 3: Millimeter Scale Attached to the Specimen
Note 4: Birefringent Plastic Bonded to the Specimen
Note 5: Photo Counter

Figure 4. Close-up of the Fatigue Crack Propagation Specimen in the IVY-12

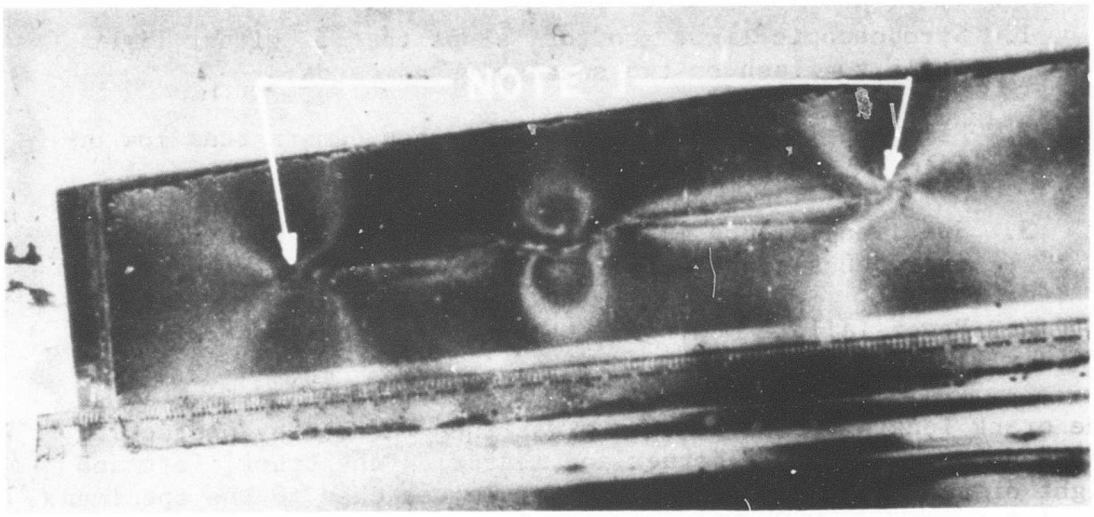

Note 1: Interference Pattern Indicating the Apex of the Fatigue Crack

Figure 5. Enlargement of One Frame of a Typical Film Strip

machine timed the photographs to the maximum alternating load, so that each picture showed the most intense possible pattern in the birefringent plastic. Other interlocks, as shown in Figure 6, are:

1. Stroboscopic light monitor; stops test if either light fails to flash on two successive commands.

2. Film supply monitor; stops test when camera runs low on film.

3. Specimen failure monitor; stops test when specimen fails or reaches a pre-set elongation.

4. Power failure monitor; stops test in the event of power loss to any system.

The crack length versus time data was then reduced by projecting the developed film on a screen and measuring the crack, left and right of center, directly from the scale attached to the specimen. Initial length, taken as a zero or tare reading, was the frame just before the frame when first growth was noted. In this manner, the crack dwell* was controlled. The right and left crack lengths and film frame number were entered on an IBM coding form.

An IBM 7094 digital computer routine was then used to calculate the following:

1. Crack length for right, left, and total.

2. Total cycles of vibratory load from the zero or tare frame.

3. Stress intensity factor, K, (psi $\sqrt{\text{inch}}$) for the right, left, and total crack.

4. Crack propagation rate (microinches per cycle) for the right, left, and total crack.

The computer output was obtained as a printed record and was also obtained as a series of punched cards which were used in further

*Crack dwell occurs when the fatigue crack does not propagate even though the applied stresses are sufficient to cause propagation normally. Residual stresses from prior loading were sufficient in this case to prevent immediate fatigue crack propagation. Crack dwell can also occur on reducing applied stresses in random or programmed testing or in propagating a fatigue crack away from a stress concentration factor.

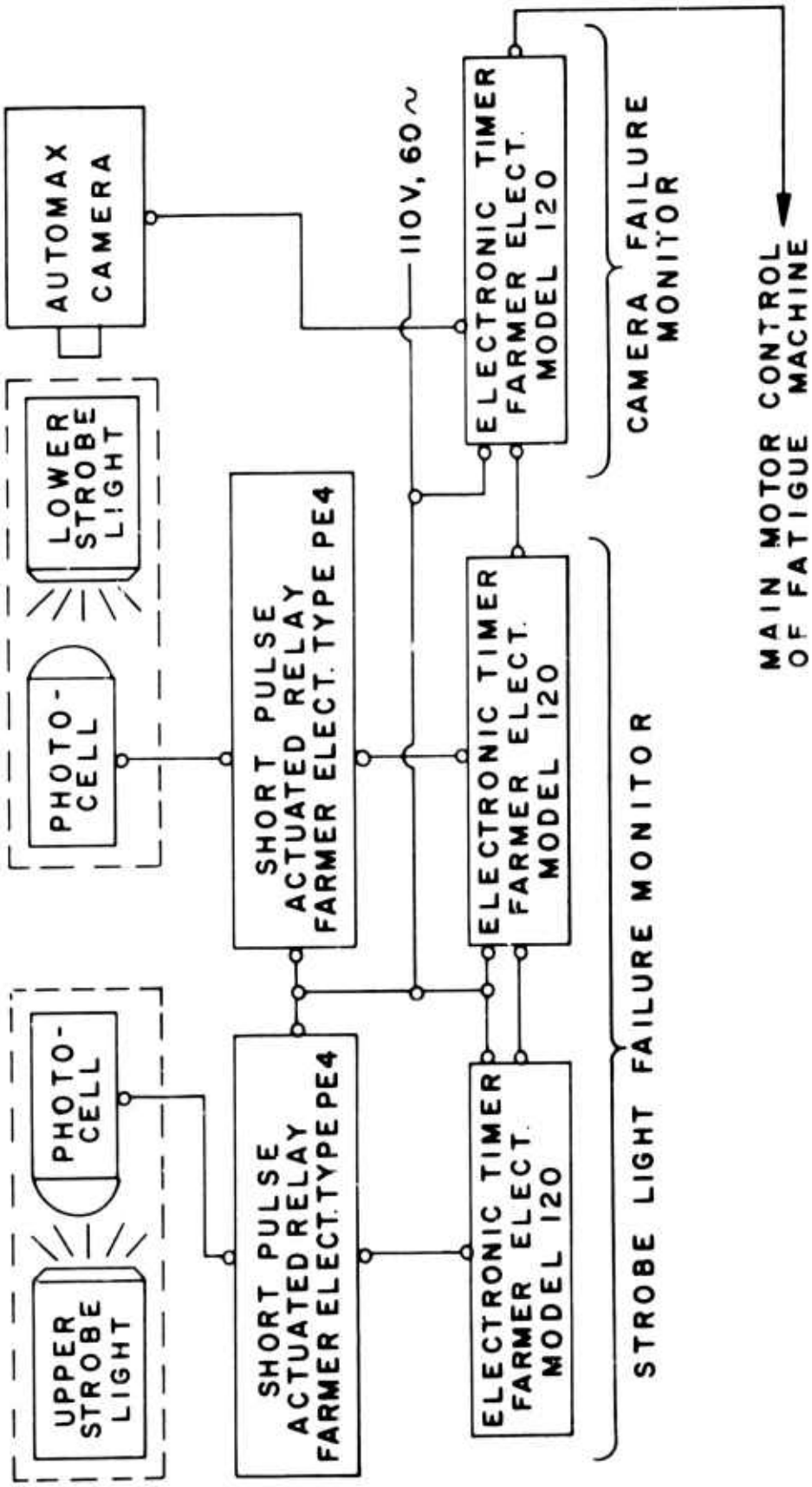

Figure 6. Schematic of the Monitoring System on the IVY-12

reduction and comparison of the data. The punched cards were used in three additional digital computer routines:

1. Plots of stress intensity factor versus fatigue crack propagation rate were obtained from an off-line plotter and a second computer routine (see Figure 7 for a typical example of this plot).

2. Plots of fatigue crack length versus number of cycles of vibratory load were obtained from the same off-line plotter and a third routine (see Figure 8 for a typical example of this plot).

3. On the plots of stress intensity factor versus fatigue crack propagation rate, a least-squares fit of the best fitting mean line was obtained for both the slow and fast propagation portions of the test data by means of a fourth digital computer routine (see Figure 9 for a typical example). This series of calculations used standard mathematical techniques based on iteration procedures which started from up to eight trial transition points between slow and fast fatigue crack propagation. Results were obtained only in a printed output form which gave the best fitting transition point as well as the equations of both the slow and fast fatigue crack propagation lines and the coordinates of the end points for both lines.

Fracture Toughness Test Procedure

The experimental procedure followed in fracture toughness testing was patterned directly after recommended standard procedures*. The fracture toughness specimen is shown in Figure 10. The width dimensions of all specimens were the same as specimens used in fatigue crack propagation tests. Fracture toughness specimens were made from the same lots and heats of material and were taken in the same orientation as the fatigue crack propagation specimens.

The center slot in the specimens was milled; rounded portions of the milled slot were filed square and notched with a power filing machine. Natural fatigue cracks were initiated at the ends of the notched slots in either an IV-4 or an IVY-12 constant load fatigue machine. Length of the cracks was controlled by the use of microwire, to obtain the 2.5-inch length shown in Figure 10.

*Recommendations of the Special Committee on Fracture Toughness Testing as stated in ASTM Special Technical Publication Number 381, Reference 3, were followed.

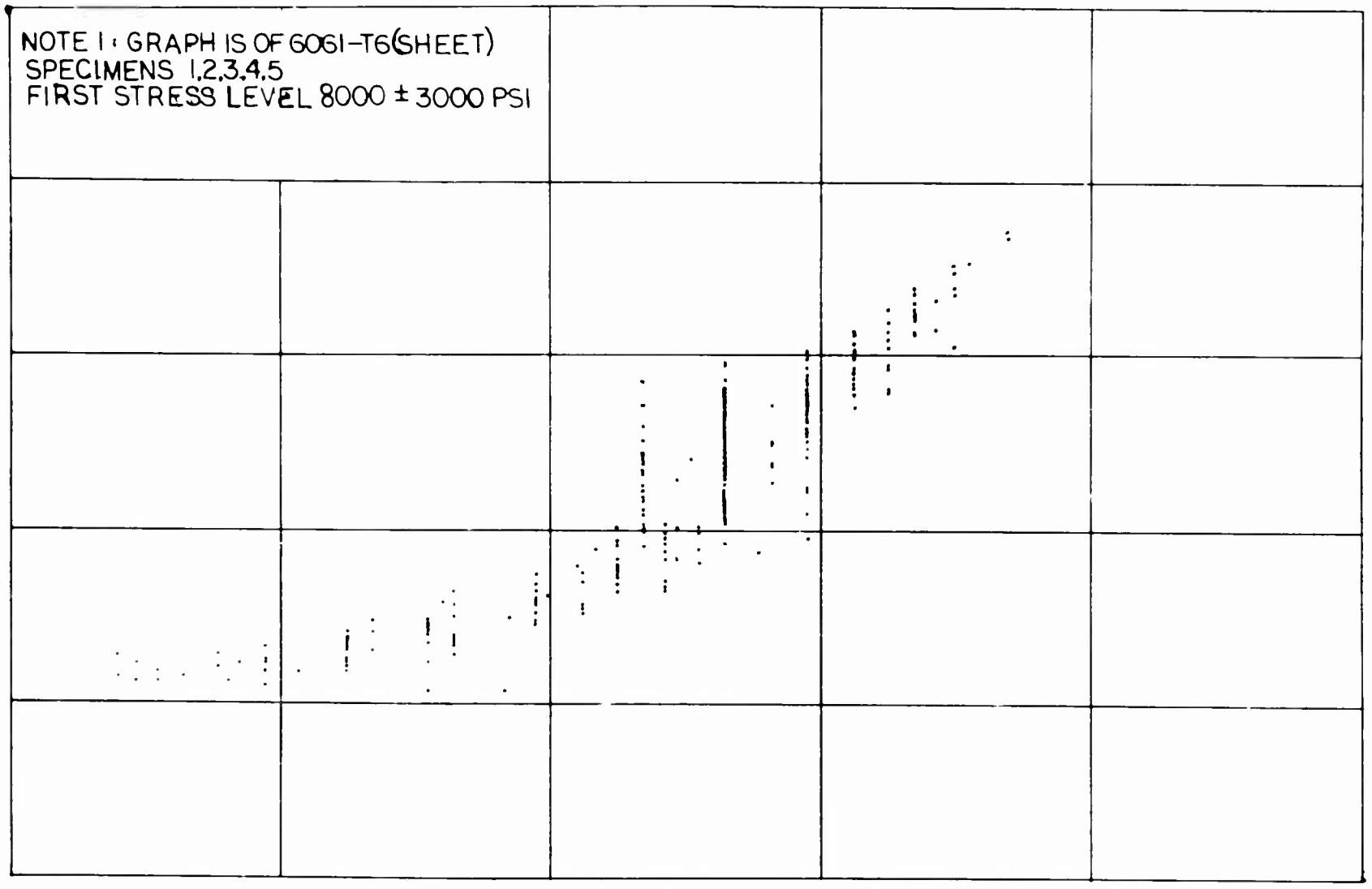

Figure 7. Typical Computer Print-Out of Stress Intensity Factor versus Crack Propagation Rate

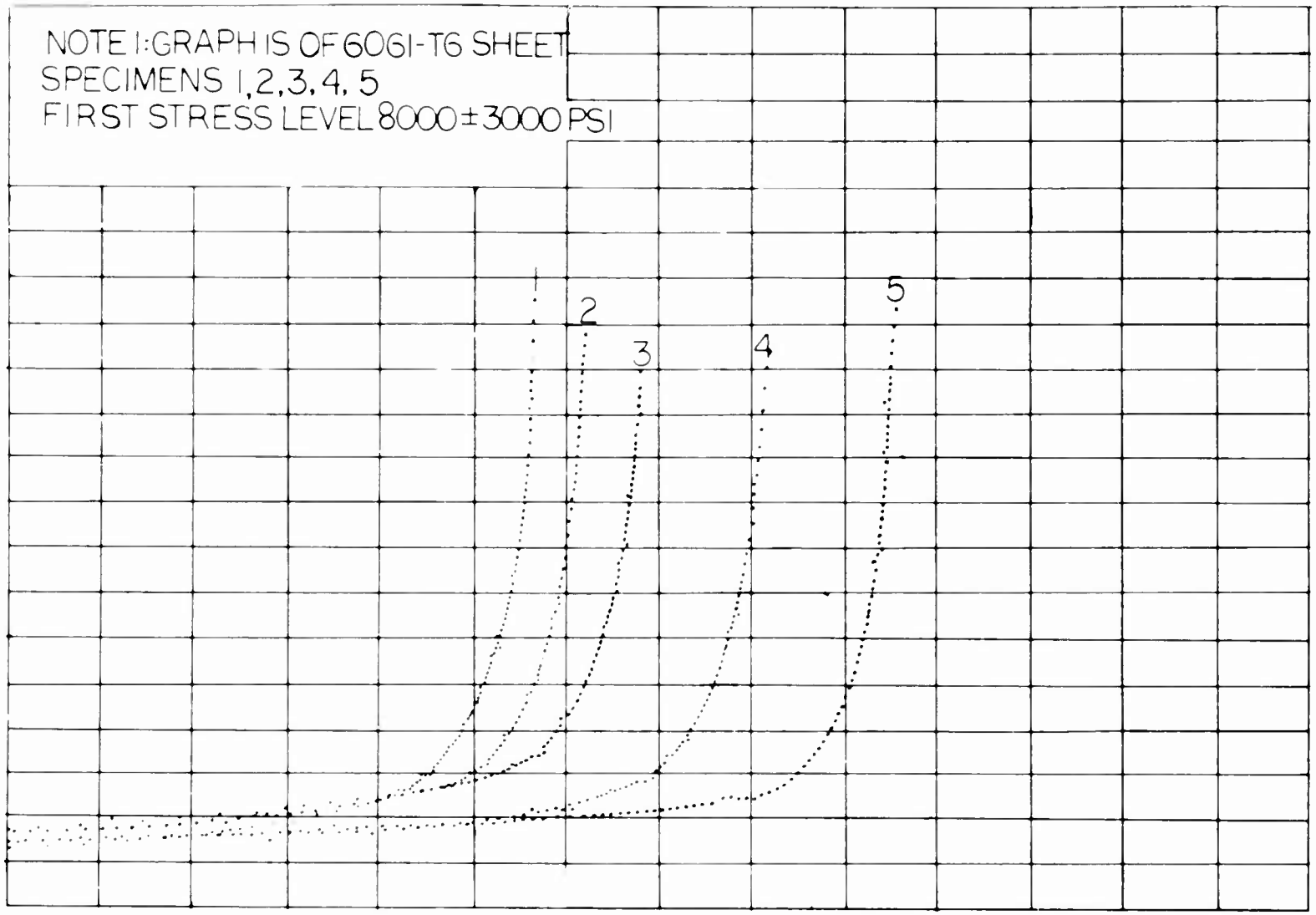

Figure 8. Typical Computer Print-Out of Crack Length versus Number of Cycles

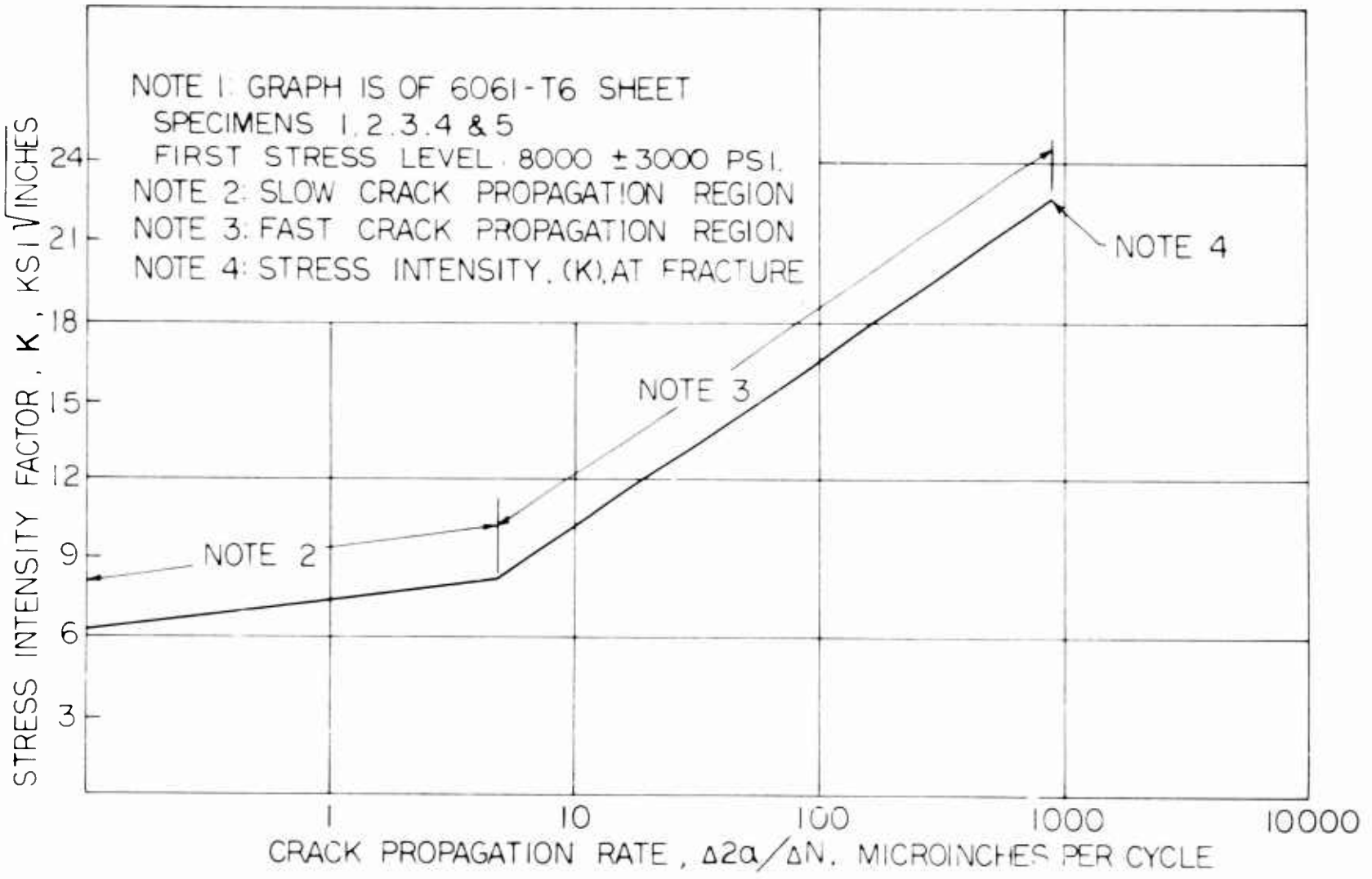

Figure 9. Typical Example of a Mean Curve of the Stress Intensity Factor versus Fatigue Crack Propagation Rate

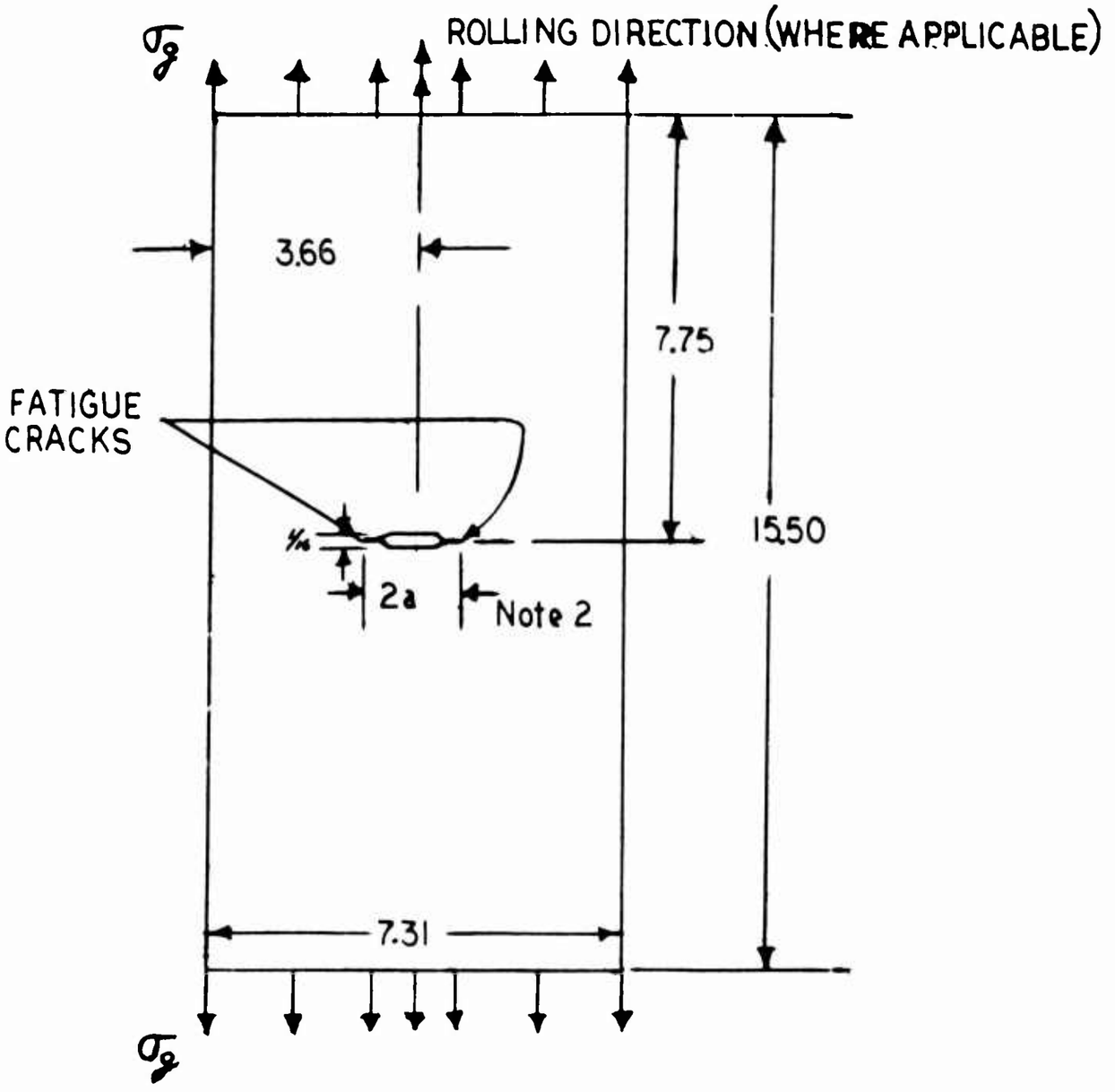

Note 1: Five-Hole Bolt Pattern Drilled (Both Ends) for Tensile Machine Fittings

Note 2: Total Length of Fatigue Crack Plus Machined Slot (2a) Was Controlled to 2.5 Inches

Figure 10. Fracture Toughness Specimen

A compliance gage, Figure 11, was used to measure crack extension by actually measuring the vertical displacement (v). This vertical displacement was converted to crack extension by the use of a calibration curve, explained later. The compliance gage, patterned after the unit described in Reference 1, converts displacement to an electrical signal, the same operating principle as an averaging extensometer used for ordinary tensile testing.

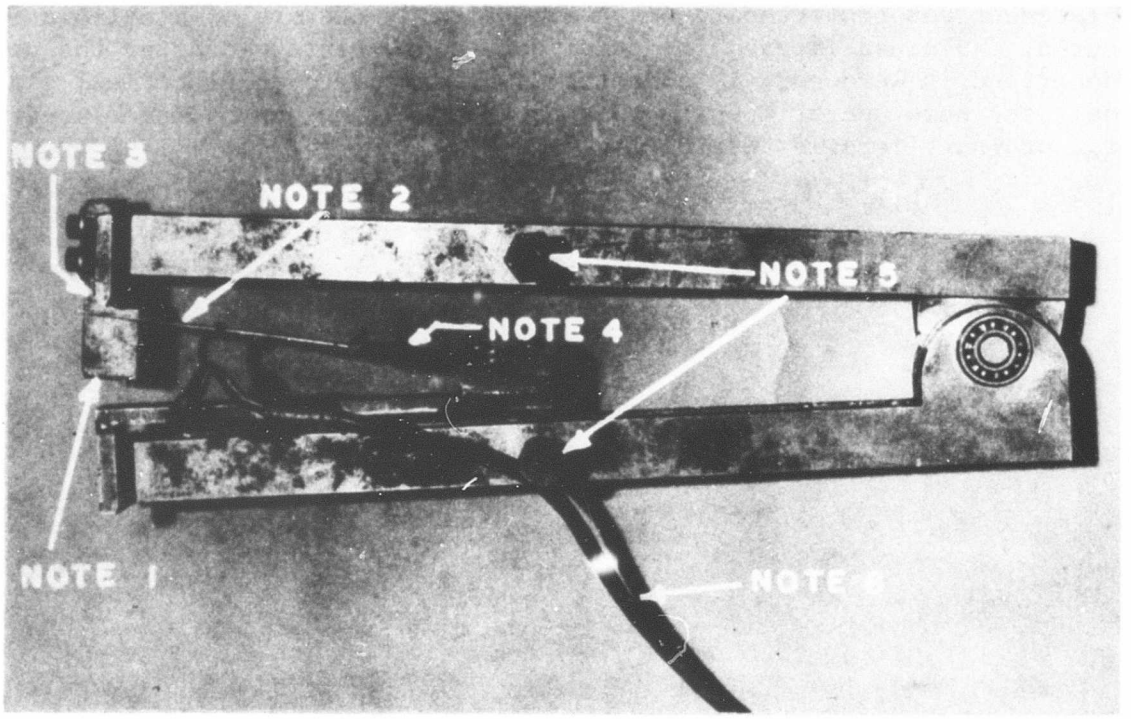

Note 1: Mechanical Stop To Prevent the Strain Gages from being Overstressed when Specimen Fails
Note 2: Knife Edge which Deflects the Cantilever Beam
Note 3: Calibrated Cantilever Beam
Note 4: Strain Gages Calibrated To Read Deflection at the Knife Edge
Note 5: Set Screws for Attaching the Gage to the Specimen
Note 6: Electrical Input from the Strain Gages to the X-Y Recorder

Figure 11. Compliance Gage

Installation of the compliance gage on a fracture toughness specimen is shown in Figure 12.

Load applied to the specimen was measured by a calibrated load cell in series with the specimen. Applied load versus displacement (v) was recorded on an X-Y recorder, Electro-Instruments Model 420. Figure 13 shows an over-all view of the test setup.

Before any testing was done, a calibration curve for the compliance gage was constructed so that the vertical displacement (v) might be converted to relative crack length. The basic calibration curve for the gage, indicated in Figure 14 as a heavy line, was drawn after load-deflection data were obtained from several aluminum (6061-T6 and 7075-T6) fracture toughness specimens under elastic loading conditions. The initial crack length (2a) in these calibration specimens ranged from 0 to 4-9/16 inches. The family of curves, shown as light lines on Figure 14, were drawn by varying the value of the modulus of elasticity in tension used in the corrected specimen compliance term (the ordinate). Figure 14 was then able to be used in fracture toughness data reduction of materials of different elastic modulii.

As explained in Reference 1, the use of the compliance gage allowed simpler data reduction. With the effect of the plastic enclave at the apex of the static crack included in the calibration of the compliance gage, the fracture toughness equation used to reduce the test data was

$$E\,G_{Ic} = (1 - \mu^2)\;K_{Ic}^2 = \sigma_g^2 \qquad w \tan\left(\pi\; a/w\right).$$

This equation was solved for K_{Ic} either at the point where the load-deflection curve deviated from a straight line or at the point of "pop-in", if "pop-in" occurred. (The term "pop-in" has been coined by other workers in the field and owes its origin to the observation that the first appreciable extension of the crack under static load is often accompanied by an audible snap from the specimen.)

At the point of maximum load (final failure), the value of K_c was calculated. But, before the K_c calculation was made, the remaining net area and net stress were calculated. The non-dimensionalized terms of corrected specimen compliance ($Ev/\sigma_g w$) and the relative crack length ($\pi\, a/w$) were calculated for the point of load deviation or "pop-in", whichever was used to determine the value of K_{Ic}. These two quantities determined a point on the calibration curve. Usually, due to variations in installation of the compliance gage, the point as determined did not lie directly on one of the curves, but lay between two of the curves calculated from the basic calibration. This point was used to determine a new curve, applicable to that

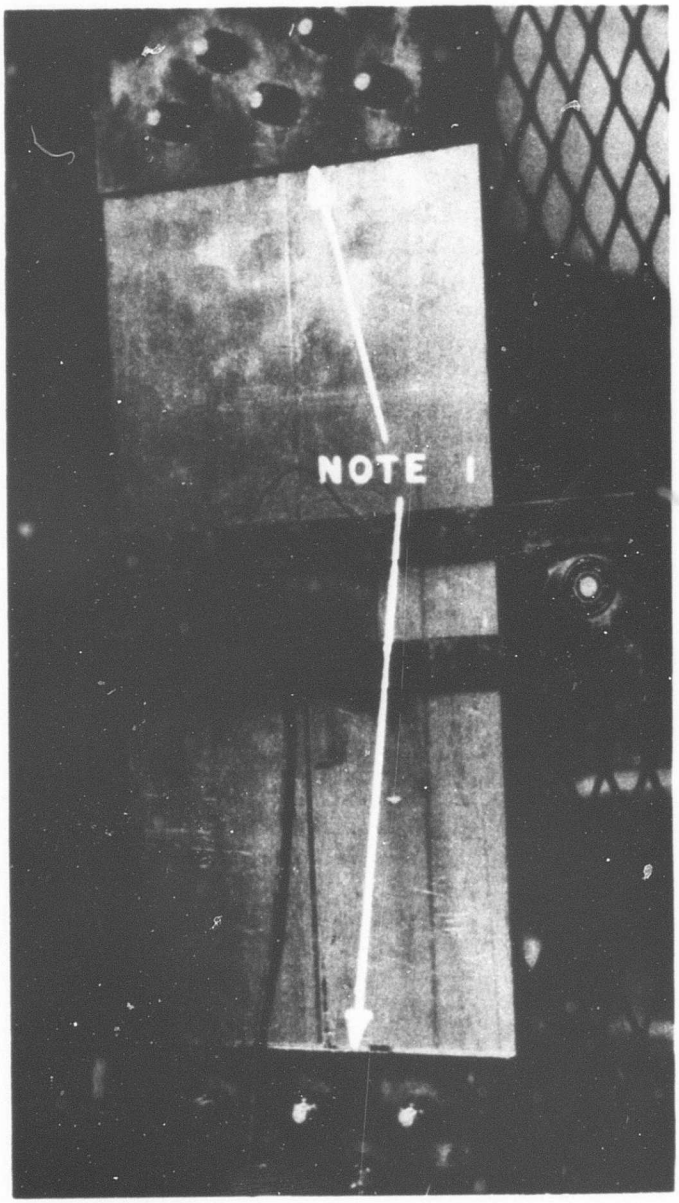

Note 1: Tensile Machine Fitting Showing the Five-Hole Bolt Pattern

Figure 12. Fracture Toughness Specimen with Compliance Gage Installed

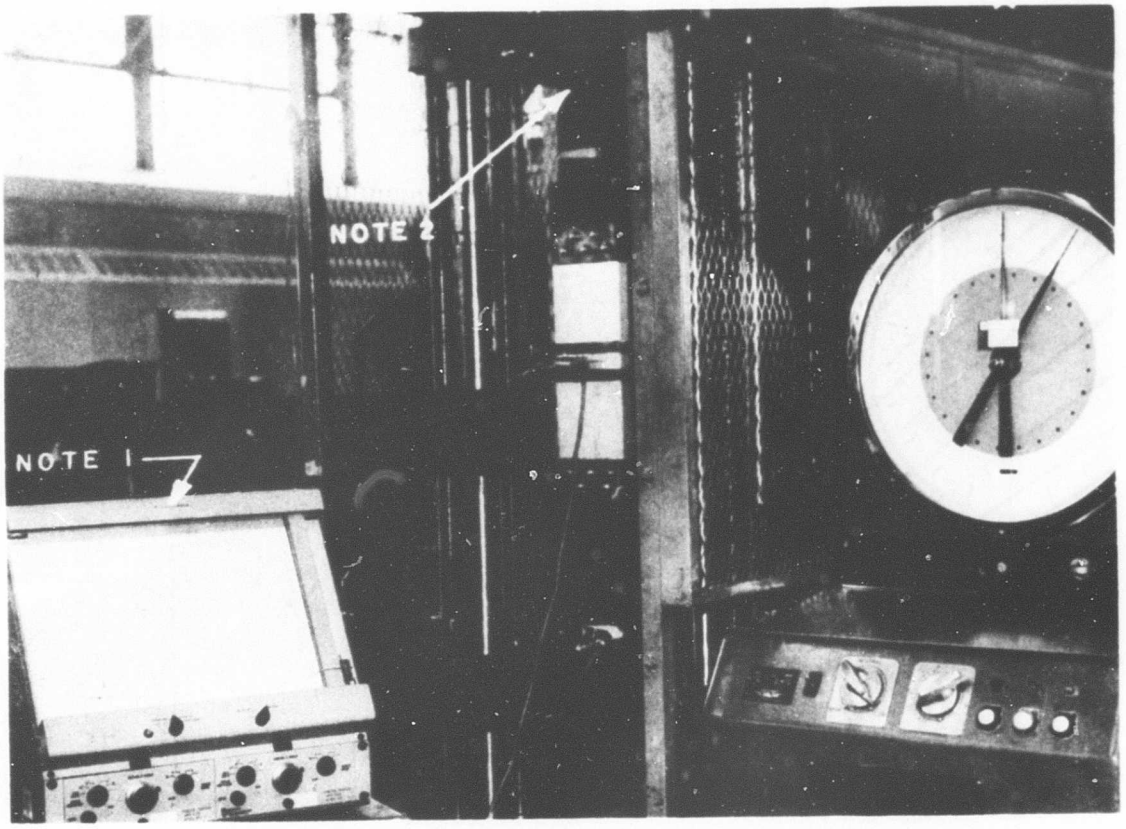

Note 1: X-Y Recorder
Note 2: Calibrated Load Cell

Figure 13. Fracture Toughness Test Setup in the Riehle Tensile Machine

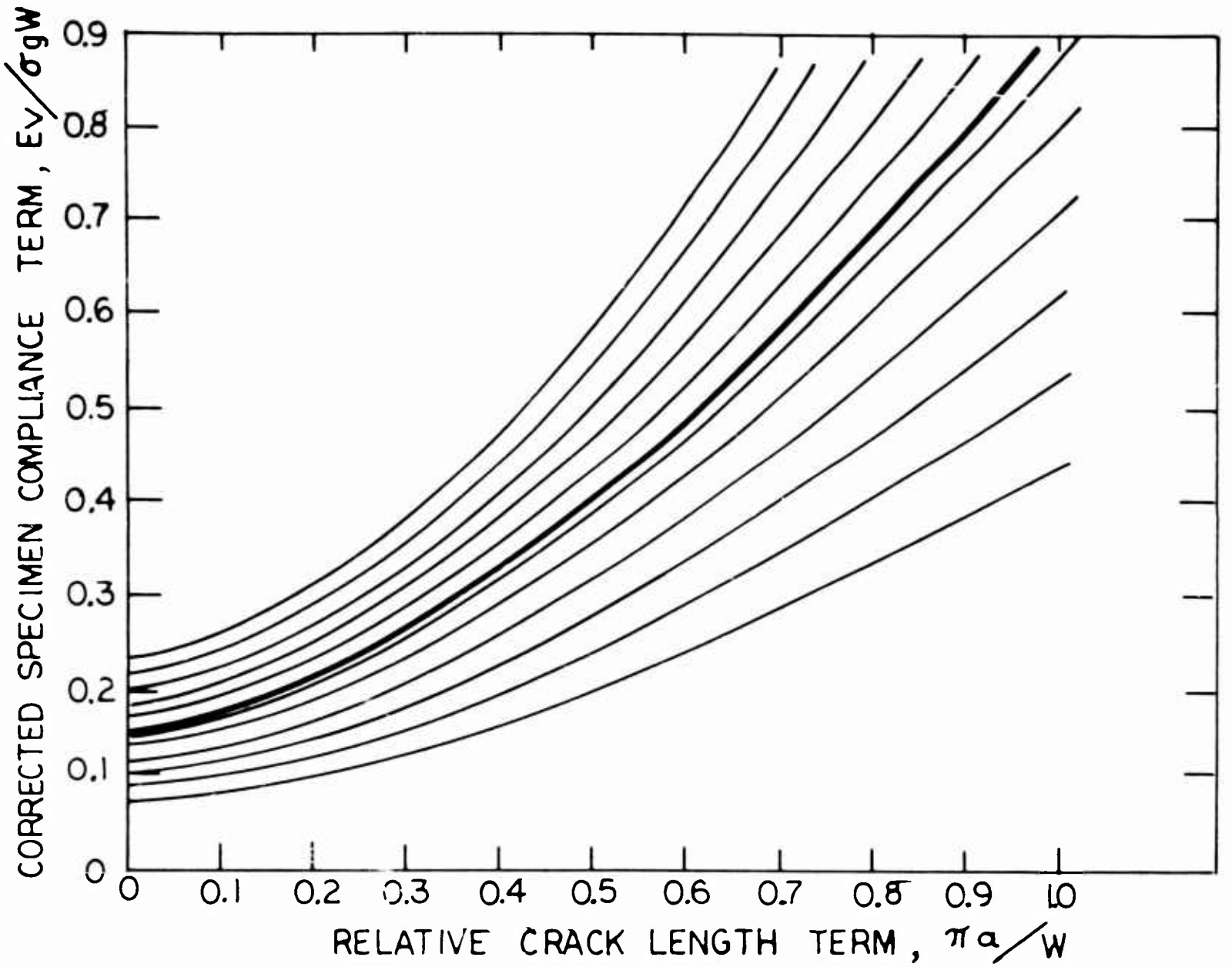

Figure 14. Compliance Gage Calibration

particular test; and with the calculated value of ($Ev/ \sigma_g w$) for the point of maximum load, the final value of (π a/w) was determined. From this (π a/w) term, the remaining net area and the net stress were calculated. If the net stress did not exceed 1.1 of the yield strength of the material, the K_c calculation was completed. But, if the net stress did exceed 1.1 of the yield strength, the calculation of K_c was not made. This is in accordance with the practice recommended by the ASTM.

When it was determined that the remaining net section of the specimen was not in a state of general yield, the value of (π a/w) was substituted directly into the equation given below and the value of K_c was determined.

$$E G_c = K_c^2 = \sigma_g^2 \; w \tan (\pi \; a/w)$$

Static Tensile Test Procedure

The test procedures outlines in Federal Test Method Standard Number 151a, "METALS; TEST METHODS", Method 211.1, "TENSION TEST", July 17, 1956, were followed without exceptions or deviations. Since the specimens were cut from sheet, plate, or machined extrusions, a flat tensile test specimen was used (type F2, shown in Figure 3 of the test method). All axial directions of all tensile test specimens corresponded to the axial directions of the fatigue crack propagation test and fracture toughness test specimens.

A Riehle Model PS-60 Universal Testing Machine was used in these tests. A two-inch Riehle extensometer and auto-graphic recorder were used to determine the yield strength of the specimens.

EXPERIMENTAL RESULTS

Fatigue Crack Propagation

Three distinct types of data presentation are used in this program. These types are:

1. Graphical presentation of stress intensity factor versus fatigue crack propagation rate (see Figure 9 for a typical example).

2. Graphical presentation of fatigue crack length versus cycles of vibratory load (see Figure 15 for a typical example).

3. Tabular presentation of the cracked life for each alloy.

For most of this report, the third type of presentation was used because of clarity and ease of presentation. In ranking materials according to their cracked life, an initial crack length of one inch was arbitrarily chosen. The initial length decision was necessary to eliminate the problems of crack dwell and initial crack length variations from specimen to specimen. Cycles to failure for this one-inch initial crack length were chosen as the figure of merit for resistance to fatigue crack propagation. Specific aspects of the fatigue crack propagation tests are:

1. Ranking of Materials:

   Tables I, II, and III list all materials and configurations tested in descending order of fatigue crack propagation resistance for each of the three test stress levels.

   Test stress levels were established on a constant stress-density basis; i.e., test stress divided by average density of the alloy system is a constant. As most common engineering materials have nearly constant ratios of elastic modulus to density, the ranking tables for tension fatigue may be used for flexure fatigue as well.

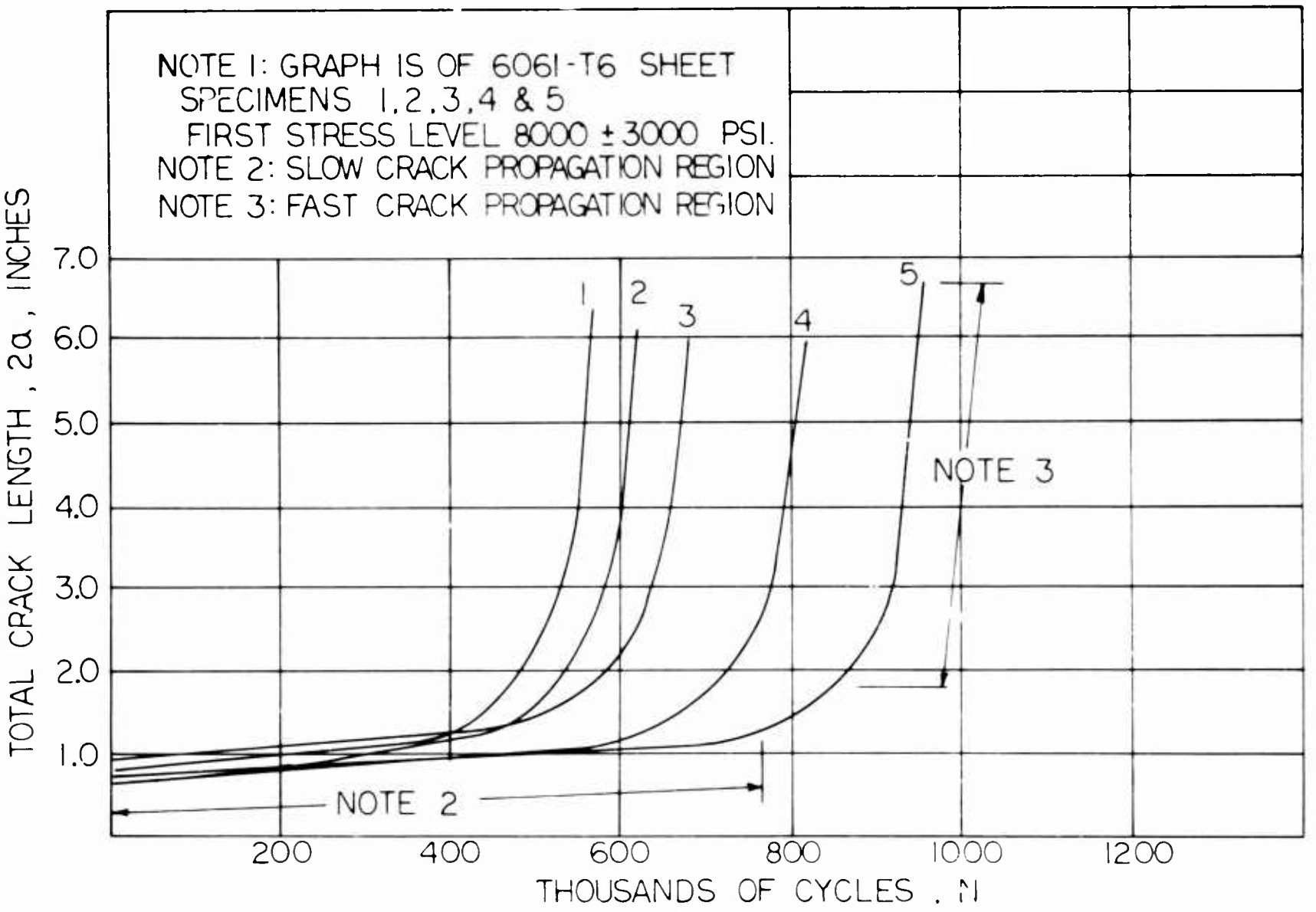

Figure 15. Typical Example of the Crack Length versus Cycles Curves

TABLE I

RANKING OF MATERIALS AT THE FIRST STRESS LEVEL*

Rank	Materials	Thickness (Inches)	Cycles to Failure x 10^3
1	6061-T6 (Ext.) (550 Shot, $15A_2$ Intensity)	.160	631
2	6061-T6 (Ext.) (230 Shot, 6A2 Intensity)	.160	551
3	2024-T3 (Chem-Milled)	.160	434
4	6061-T6 (Ext.)	.325	423
5	6061-T4 (Plate)	.160	405
6	4340 (150 ksi) (330 Shot, $7A_2$ Intensity)	.063	399
7	6061-T6 (Ext.)	.080	390
8	2024-T4	.160	362
9	6061-T6 (Sheet)	.160	316
10	Ti-8Al-1Mo-1V	.090	301
11	4130 (150 ksi)	.063	299
12	6061-T6 (Ext.) (Dodecyl Alcohol Spray)	.160	290
13	4340 (150 ksi) (110 Shot, $5A_2$ Intensity)	.063	272
14	6061-T6 (Ext.)	.160	260
15	4340 (150 ksi)	.090	250
16	Ti-6Al-4V	.045	233
17	6061-T6 (Ext.) (Water Spray)	.160	222
18	301 (1/4 Hard)	.063	221
19	2024-T3	.160	215
20	7075-T4	.160	215
21	410 (Condition "T")	.063	204
22	4340 (125 ksi)	.063	197
23	2024-T6	.160	195
24	4340 (150 ksi) (Dodecyl Alcohol Spray)	.063	195
25	4340 (150 ksi) (Water Spray)	.063	181
26	4340 (150 ksi)	.125	177
27	4340 (150 ksi)	.063	176
28	18% Ni Maraging Steel 250 ksi)	.063	145
29	7001-T75	.160	126
30	4340 (200 ksi)	.063	115

TABLE I (contd.)

Rank	Materials	Thickness (Inches)	Cycles to Failure x 10^3
31	7075-T6	.160	114
32	Ti-6Al-4V	.090	113
33	Ti-5Al-2.5Sn	.063	98
34	Ti-6Al-4V	.063	95
35	Ti. Comm. Pure	.090	88
36	Ti 140A	.090	83
37	HK31A-H24	.160	70
38	AZ91C-T6	.160	68
39	7178-T6	.160	28

*First gross stress levels (σ_g) are:

Steel	+23,000	$\pm$8,700 psi
Titanium	+13,400	$\pm$5,000 psi
Aluminum	+ 8,000	$\pm$3,000 psi
Magnesium	+ 5,400	$\pm$2,030 psi

TABLE II

RANKING OF MATERIALS AT THE SECOND STRESS LEVEL*

Rank	Materials	Thickness (Inches)	Cycles to Failure x 10^3
1	6061-T6 (Ext.) (550 Shot, $15A_2$ Intensity)	.160	130
2	6061-T6 (Ext.) (230 Shot, $6A_2$ Intensity)	.160	121
3	6061-T6 (Ext.)	.080	101
4	6061-T4 (Plate)	.160	98
5	6061-T6 (Ext.)	.160	79
6	2024-T4	.160	77
7	6061-T6 (Ext.)	.325	76
8	2024-T3 (Chem-Milled)	.160	66
9	6061-T6 (Sheet)	.160	57
10	Ti-8Al-1Mo-1V	.090	56
11	Ti-6Al-4V	.045	54
12	6061-T6 (Ext.) (Water Spray)	.160	54
13	4340 (150 ksi) (330 Shot, 7A Intensity)	.063	53
14	4340 (150 ksi)	.090	52
15	301 (1/4 Hard)	.063	52
16	4130 (150 ksi)	.063	49
17	410 (Condition "T")	.063	48
18	18% Ni Maraging Steel (250 ksi)	.063	48
19	4340 (125 ksi)	.063	48
20	4340 (150 ksi) (110 Shot, 5A Intensity)	.063	47
21	Ti-6Al-4V	.090	44
22	Ti 140A	.090	43
23	2024-T6	.160	43
24	6061-T6 (Ext.) (Dodecyl Alcohol Spray)	.160	38
25	Ti-6Al-4V	.063	36
26	2024-T3	.160	36
27	4340 (150 ksi)	.125	35
28	7075-T4	.160	33
29	4340 (150 ksi) (Dodecyl Alcohol Spray)	.063	33
30	4340 (150 ksi) (Water Spray)	.063	29

TABLE II (contd.)

Rank	Materials	Thickness (Inches)	Cycles to Failure x 10^3
31	Ti. Comm. Pure	.090	28
32	4340 (150 ksi)	.063	26
33	HK31A-H24	.160	26
34	4340 (200 ksi)	.063	25
35	Ti-5Al-2.5Sn	.063	19
36	7075-T6	.160	18
37	7001-T75	.160	17
38	7178-T6	.160	9
39	AZ91C-T6	.160	3

*Second gross stress levels (σ_g) are:

Steel	+23,000 $\pm$17,400 psi
Titanium	+13,400 $\pm$10,000 psi
Aluminum	+ 8,000 $\pm$ 6,000 psi
Magnesium	+ 5,400 $\pm$ 4,060 psi

TABLE III

RANKING OF MATERIALS AT THE THIRD STRESS LEVEL*

Rank	Materials	Thickness (Inches)	Cycles to Failure x 10^3
1	6061-T6 (Ext.)	.160	456
2	6061-T6 (Sheet)	.160	453
3	2024-T3	.160	411
4	6061-T6 (Ext.) (230 Shot, $6A_2$ Intensity)	.160	382
5	6061-T6 (Ext.) (Dodecyl Alcohol Spray)	.160	373
6	6061-T6 (Water Spray)	.160	354
7	410 (Condition "T")	.063	349
8	6061-T6 (Ext.) (550 Shot, $15A_2$ Intensity)	.160	336
9	2024-T3 (Chem-Milled)	.160	328
10	Ti-6Al-4V	.090	325
11	2024-T4	.160	318
12	6061-T4 (Sheet)	.160	274
13	4340 (150 ksi) (330 Shot, $7A_2$ Intensity)	.063	239
14	4340 (150 ksi) (Dodecyl Alcohol Spray)	.063	219
15	4340 (125 ksi)	.063	213
16	Ti-8Al-1Mo-1V	.090	207
17	4340 (150 ksi) (110 Shot, $5A_2$ Intensity)	.063	205
18	301 (1/4 Hard)	.063	197
19	4340 (150 ksi) (Water Spray)	.063	193
20	2024-T6	.160	191
21	4130 (150 ksi)	.063	188
22	Ti-5Al-2.5Sn	.063	188
23	4340 (150 ksi)	.063	141
24	4340 (200 ksi)	.063	139
25	Ti. Comm. Pure	.090	131
26	HK31A-H24	.160	120
27	7075-T4	.160	110
28	18% Ni Maraging Steel (250 ksi)	.063	106

TABLE III (contd.)

Rank	Materials	Thickness (Inches)	Cycles to Failure x 10^3
29	Ti 140A	.090	106
30	7075-T6	.160	81
31	7178-T6	.160	35
32	AZ91C-T6	.160	14

*Third gross stress levels (σ_g) are:

Steel	+34,500	$\pm$8,700 psi
Titanium	+20,000	$\pm$5,000 psi
Aluminum	+12,000	$\pm$3,000 psi
Magnesium	+ 8,100	$\pm$2,030 psi

All aspects of the test program are included in materials ranking. As a result, shot-peening effects (cold work), thickness effects, metallurgical effects (heat treatment), and chemical effects (water and dodecyl alcohol) are all ranked against each other in the same tables. These additional effects are:

2. Thickness Effect:

   At the inception of this program, examination of the "tunneling" action of fatigue "beach-marks" in heavy sections led to the belief that thicker sections would exhibit less resistance to fatigue crack propagation. Corollary to this was the belief that free surfaces acted as fatigue crack propagation retardants and that cold-work of these surfaces would act as a retardant (see discussion below).

   Although the largest possible ranges of thickness of specimens were tested, little or no difference in resistance to fatigue crack propagation was observed in this test series. This is apparent from both the ranking of materials, Tables I, II, and III, and the plots of stress intensity factor versus fatigue crack propagation rate, none of which indicate any measurable effect for the thickness ranges of aluminum (0.080 - 0.160 - 0.325 inch), steel (0.063 - 0.090 - 0.125 inch), or titanium (0.045 - 0.063 - 0.090 inch).

3. Effect of Cold Work:

   Surfaces of aluminum and steel alloys tested in this series were shot-peened to two different intensities (each) to determine the relative effect of shot-peening intensity on the resistance to fatigue crack propagation. Shot-peening conditions, chosen for the greatest range of practical interest, Reference 6, were:

   A. 6061-T6 (extruded) aluminum
      a. 230 shot, 6A2 intensity
      b. 550 shot, 15A2 intensity

   B. 4340 (150 ksi) steel
      a. 110 shot, 5A2 intensity
      b. 330 shot, 7A2 intensity

   Both materials showed improvement in resistance to fatigue crack propagation as a result of shot-peening. The more intense peening resulted in a greater increase in resistance in both cases. Steel exhibited a greater relative increase in resistance than aluminum did.

Figure 16 shows plots of stress intensity factor versus fatigue crack propagation rate for as-rolled and shot-peened steel. In both the slow and fast crack propagation regions, a larger stress intensity factor is needed on shot-peened steel to obtain the same crack propagation rate. At the transition point between slow and fast crack propagation, the stress intensity factor is not significantly different for any surface condition. However, the propagation rate is lower for shot-peened specimens.

The stress intensity factor at static failure is lower for the shot-peened steel. This is apparently due to the residual tensile stress in the core of the sheet adding to the applied stress. The length of the fatigue crack at the time of static failure of the shot-peened specimens is correspondingly shorter. This reduction is not considered significant in considering the cracked life of a shot-peened component, as it occurs very close to the point of static failure.

It is generally agreed that the increase in resistance to fatigue crack propagation is the result of the residual compressive stresses in the surface rather than cold work. This research is far from complete, since the full range of peening intensities has not been investigated and the effects of cyclic-induced stress relaxation (sometimes called fading) reported by some researchers and not found by others has not been investigated. Shot-peening also increases crack dwell time.

4. Metallurgical Effects:

As can be seen from Tables I, II, and III, one very definite general trend exists. The more ductile, tougher materials, in general, those of lower tensile strengths, are more resistant to fatigue crack propagation. This is most readily seen in the case of 4340 steel, tested at strength levels of 125, 150, and 200 ksi ultimate tensile strength. At the same test levels, the higher the ultimate tensile strength, the lower the resistance to fatigue crack propagation.

This same general trend can also be found in the cases of 6061-T4 and -T6, 2024-T3, -T4, -T6, and 7075-T4 and -T6.

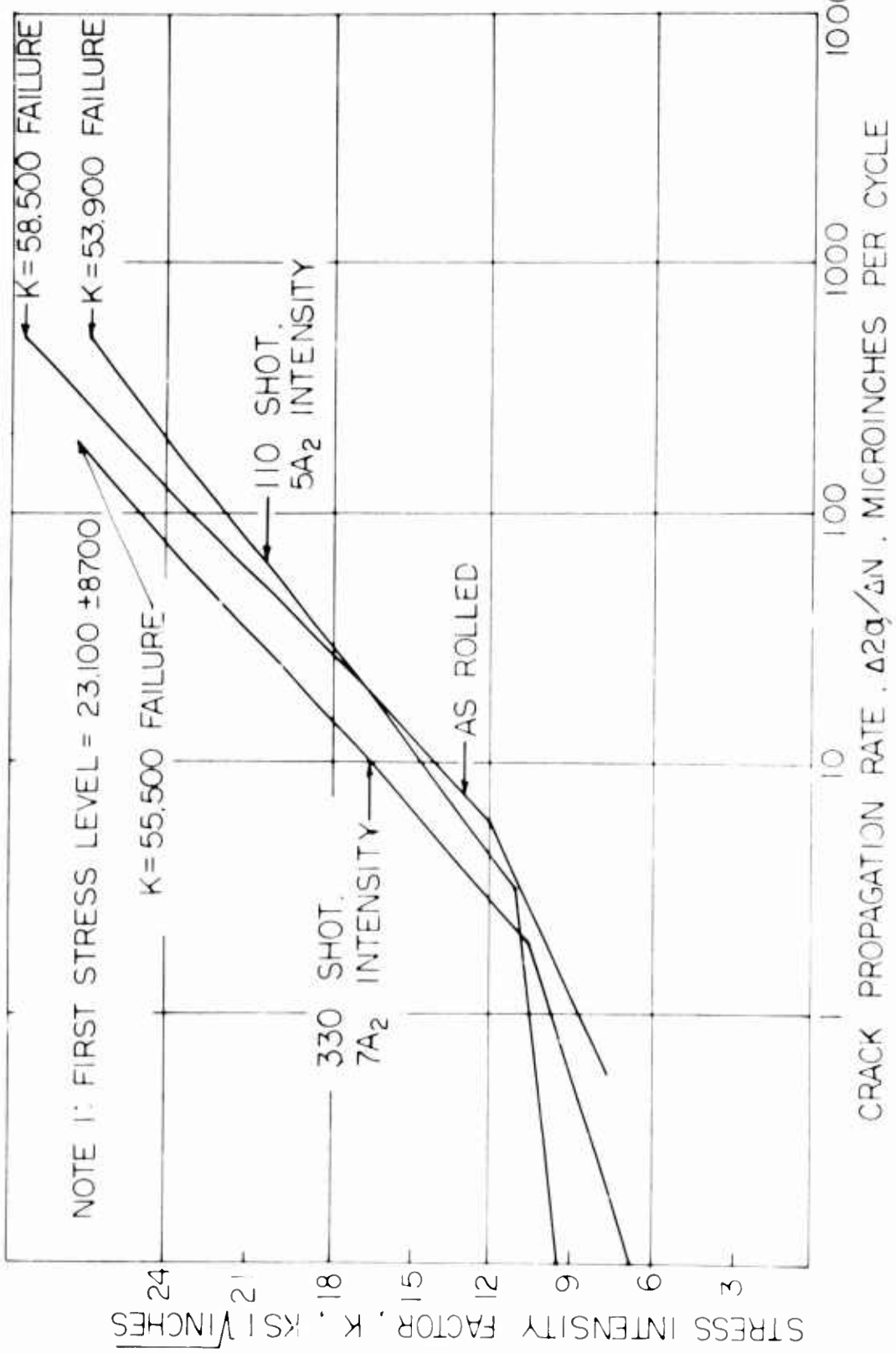

Figure 16. Effect of Shot-Peening on 4340 Steel

5. Effect of Chemicals:

Fatigue crack propagation tests were conducted with both distilled water and dodecyl alcohol (chemically pure) sprayed against the opposite side of the specimen to that photographed by the time-lapse camera. The test setup is shown in Figure 17.

As a result of the research conducted by Frankel, Bennett, and Holshauser, Reference 4, it was expected that an improvement would be seen in the resistance to fatigue crack propagation of materials sprayed with dodecyl alcohol. Instead, both distilled water and dodecyl alcohol lowered the fatigue crack propagation resistance of aluminum and steel by approximately the same amount. Research completed by Christensen, Reference 2, has indicated a possible mechanism which could explain the change in cracked life which occurs when the specimen surface is directly impinged by a fluid. Although Christensen's research was applied to an opening and closing crack, a fluid wedge in a partially closing crack could cause the reduction observed in these tests. This reasoning is further strengthened by direct observation of a pumping action from the fatigue crack of both liquids as the final failure point was approached.

An additional chemical action was investigated in these series: chemically milled 2024-T3 aluminum alloy. The 2024-T3 sheet was chemically milled in an alkaline chemical milling bath, removing 0.015 inch of material from both sides, with a final surface finish of 10 RMS. No significant change in the resistance to fatigue crack propagation was found for this condition.

6. Laminated Plastics:

Test results of plastic laminates indicate only that considerable research is necessary in this field. The data obtained in this test series is not recommended for design application for the following reasons:

A. The derivation of the formulae for calculation of fracture toughness parameters assumes homogeneous, isotropic media. Laminates are not in this category. It is not possible within the limits of this test series to determine the effect on the reliability of the data of this basic difference.

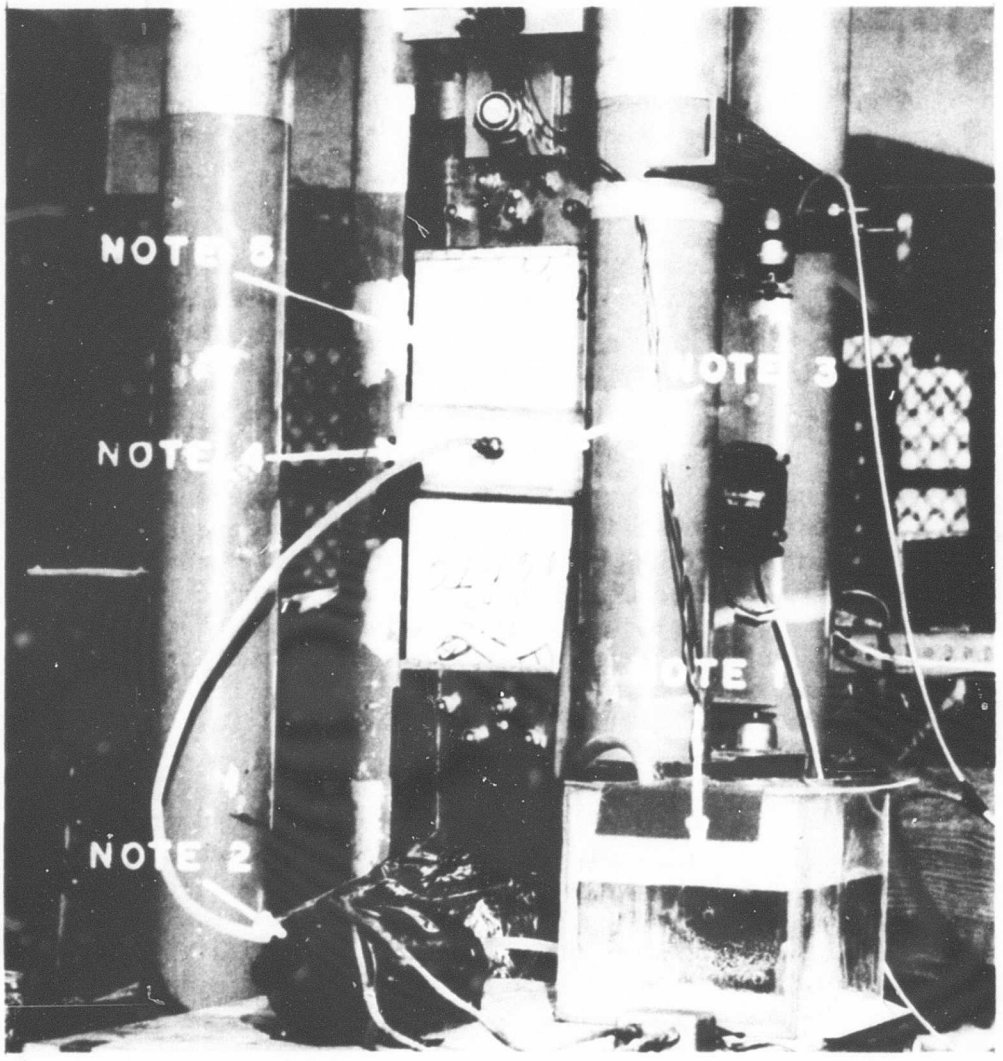

Note 1: Plastic Container Used as a Reservoir
Note 2: 28-Volt DC Motor - Pump Combination
Note 3: Plastic Container Used To Collect the Sprayed Liquid and Return it to the Reservoir
Note 4: Spray Nozzle
Note 5: Fatigue Crack Propagation Specimen

Figure 17. Chemical Effect Test Setup

B. Researchers in fatigue of metallic materials have developed certain standard techniques, one of which is the "probit" method. The probit test is used to determine stress levels to be used in a fatigue test program, and consists of applying a fatigue load, estimated to be too low for failure, to a specimen for approximately one million cycles, increasing the load for another million cycles, increasing the load a second time, a third time, etc., until the specimen fails. The S/N fatigue curve data points are then found by testing specimens at a single stress derived from the probit failure stress. It has been observed that metallic probit specimens fail at a stress level approximately 5 to 10% above that of a virgin specimen. This increase has been named "coaxing effect".

Probit tests were not satisfactory on laminates, as may be seen in Table IV. Probit #1 failed at the third stress level, but probit #2 required an even higher stress level for failure, while probit #3 and 5 specimens required an 8-1/2% higher stress for failure. The laminates exhibit a "negative coaxing effect". This was found on all laminates tested.

TABLF IV

PROBIT TEST RESULTS FOR 181/150
GLASS CLOTH LAMINATES (WARP DIRECTION)

Specimen	Stress Level	Cycles of Load	Comments
Probit #1	5,480 ± 2,055 psi	$3,000 \times 10^3$	No Crack Growth
	5,985 ± 2,245 psi	$3,000 \times 10^3$	No Crack Growth
	6,490 ± 2,435 psi	$1,548 \times 10^3$	Failed
Probit #2	6,490 ± 2,435 psi	$4,700 \times 10^3$	No Crack Growth
	6,995 ± 2,625 psi	$1,270 \times 10^3$	Failed
Probit #3	7,500 ± 2,815 psi	$1,500 \times 10^3$	Failed
Specimens 1 - 5	7,500 ± 2,815 psi	Av. $2,286 \times 10^3$ Stn'd Dev. $1,881 \times 10^3$	

Although cumulative fatigue damage or "negative coaxing" is the only form of stress history investigated in this program, other work indicates that prior stresses due to quasi-static loading, random fatigue loading, thermal shock, and alternate freeze-thaw, among others, also affect the specimen fatigue strength of laminates. Considerably more work must be done to rationalize the fatigue characteristics of laminates.

Stress levels determined by probit tests for fatigue crack propagation tests are listed in Table V. Only the lowest test stress level was determined by probit testing. The two higher test stress levels were determined in the same manner as the tests of metallics.

TABLE V

FATIGUE CRACK PROPAGATION TEST STRESS LEVELS FOR GLASS CLOTH LAMINATES

Specimen	Stress Level	Determined by	Notes
181 glass cloth, loaded in warp direction	7500 ± 2815	probit	
	7500 ± 5630	calculation	
	11250 ± 2815	calculation	
181 glass cloth, loaded at 45° to warp direction	5560 ± 2084	probit	
	5560 ± 4168	calculation	1
	8300 ± 2084	calculation	
143 glass cloth, loaded in warp direction	10800 ± 4075	probit	
	10800 ± 8150	calculation	
	16200 ± 4075	calculation	2
143 glass cloth, loaded in fill direction	3030 ± 1135	probit	
	3030 ± 2270	calculation	
	4550 ± 1135	calculation	
143 glass cloth, loaded at 45° to warp direction	4940 ± 1845	probit	
	4940 ± 3690	calculation	
	7400 ± 1845	calculation	

Note 1: Specimens at this load failed too fast to obtain crack propagation data.

Note 2: Specimens at this load elongated (permanently) without propagating the fatigue crack, so that no fatigue crack propagation data was obtained.

Fracture Toughness Tests:

The fracture toughness results are reported in Table VI. K_{Ic} was obtained for all materials tested, but it was generally not possible to calculate K_c. For most of the common engineering materials considered in this study, general yield occurred across the net section before brittle fracture could occur. With general yield, fracture toughness no longer applies as a physical description of the failure, and therefore, the K_c value could not be validly calculated.

In all cases, K_{Ic} was numerically larger than the maximum K calculated at or near failure in fatigue crack propagation tests of the same materials. Although many of the fatigue crack propagation specimens were not run to complete failure bacause of the amplitude limits of the fatigue test machines, all specimens were tested to the point where the fatigue crack propagation could be described as delayed static failure. At this point, the fatigue crack propagation was extremely fast, with the length versus cycles curve becoming nearly asymptotic, an infinite change in length for an infinitesimal increase in cycles of applied stress. Consequently, it is felt that the error is negligible in defining the final stress intensity factor obtained in fatigue crack propagation tests as the stress intensity factor for brittle static failure of the specimen.

Comparison of the values of stress intensity factor obtained from fracture toughness tests and from the final static fracture of fatigue crack propagation tests required an adjustment in the test data. The adjustment was necessary due to the difference in mathematical models used to represent the change in stress concentration factor of the crack as the crack length increased across the finite-width specimen. This correction has been referred to as a geometric correction factor, indicating the fundamental relation between crack length and the finite specimen width.

The problem of the mathematical model used to represent the change in the stress concentration factor of the crack as the crack length changes has been, and still is, a subject of much discussion in the literature. The measure of accuracy of these proposed models has always been correlation with test data, and each author shows a very good fit with the test data, for his model.

TABLE VI

FRACTURE TOUGHNESS TEST RESULTS

	Thickness (inches)	K_c* (psi $\sqrt{in}$)	K_{Ic}** (psi $\sqrt{in}$)	K_{Ic}*** (psi $\sqrt{in}$)	K**** (psi $\sqrt{in}$)
I. Ranking of Materials					
A. Aluminum					
1. 6061-T6 (sheet)	0.160	-	25,000	34,000	
+ 8,000 ± 3,000 psi					21,000
+ 8,000 ± 6,000 psi					26,300
+ 12,000 ± 3,000 psi					28,800
2. (a) 2024-T3	0.160	-	26,200	35,000	
+ 8,000 ± 3,000 psi					20,500
+ 8,000 ± 6,000 psi					19,500
+ 12,000 ± 3,000 psi					24,700
(b) 2024-T4	0.160	-	22,300	30,000	
+ 8,000 ± 3,000 psi					20,300
+ 8,000 ± 6,000 psi					23,000
+ 12,000 ± 3,000 psi					25,700
(c) 2024-T6	0.160	-	22,200	30,000	
+ 8,000 ± 3,000 psi					18,600
+ 8,000 ± 6,000 psi					22,400
+ 12,000 ± 3,000 psi					26,300
3. 7075-T6	0.160	58,150	26,000	34,000	
+ 8,000 ± 3,000 psi					17,000
+ 8,000 ± 6,000 psi					21,600
+ 12,000 ± 3,000 psi					23,300

TABLE VI (contd.)

Item	Thickness (inches)	K_c* (psi $\sqrt{in}$)	K_{Ic}** (psi $\sqrt{in}$)	K_{Ic}*** (psi $\sqrt{in}$)	K**** (psi $\sqrt{in}$)
4. 7178-T6	0.160	41,370	20,400	27,000	
+ 8,000 ±3,000 psi					15,600
+ 8,000 ±6,000 psi					15,200
+12,000 ±3,000 psi					19,000
5. 7001-T75	0.160	34,400	21,800	29,000	
+ 8,000 ±3,000 psi					14,200
+ 8,000 ±6,000 psi					16,000
B. Steel					
1. 4130 (150 ksi)	0.063	-	82,300	112,000	
+23,100 ± 8,700 psi					53,800
+23,100 ±17,400 psi					62,500
+34,500 ± 8,700 psi					71,000
2. 4340 (150 ksi)	0.063	-	112,000	150,000	
+23,100 ± 8,700 psi					58,500
+23,100 ±17,400 psi					62,900
+34,500 ± 8,700 psi					77,400
3. 301 (1/4 Hard)	0.063	-	75,900	103,000	
+23,100 ± 8,700 psi					60,800
+23,100 ±17,400 psi					82,000
+34,500 ± 8,700 psi					78,400

TABLE VI (contd.)

Item	Thickness (inches)	K_c* (psi $\sqrt{in}$)	K_{Ic}** (psi $\sqrt{in}$)	K_{Ic}*** (psi $\sqrt{in}$)	K**** (psi $\sqrt{in}$)
4. 410 (Condition "T")	0.063	-	96,800	129,000	
+23,100 ± 8,700 psi					56,500
+23,100 ±17,400 psi					72,200
+34,500 ± 8,700 psi					77,400
5. 18% Ni Maraging Steel (250 Grade)	0.063	155,000	123,000	168,000	
+23,100 ± 8,700 psi					59,700
+23,100 ±17,400 psi					69,700
+34,500 ± 8,700 psi					67,300
C. Titanium					
1. (Ti-140A)	0.090	-	52,700	72,000	
+13,400 ± 5,000 psi					29,600
+13,400 ±10,000 psi					37,700
+20,000 ± 5,000 psi					45,300
2. Commercially Pure	0.090	-	45,000	59,000	
+13,400 ± 5,000 psi					36,300
+13,400 ±10,000 psi					44,400
+20,000 ± 5,000 psi					47,000

TABLE VI (contd.)

Item	Thickness (inches)	K_c* (psi $\sqrt{in}$)	K_{Ic}** (psi $\sqrt{in}$)	K_{Ic}*** (psi $\sqrt{in}$)	K**** (psi $\sqrt{in}$)
3. 8Al-1Mo-1V	0.090	-	53,400	72,500	
+13,400 ± 5,000 psi					28,200
+13,400 ±10,000 psi					42,000
+20,000 ± 5,000 psi					44,400
4. 6Al-4V	0.090	169,000	55,300	75,000	
+13,400 ± 5,000 psi					25,600
+13,400 ±10,000 psi					40,000
+20,000 ± 5,000 psi					43,000
5. 5Al-2.5Sn	0.063	-	74,000	100,000	
+13,400 ± 5,000 psi					31,300
+13,400 ±10,000 psi					41,500
+20,000 ± 5,000 psi					44,200
D. Magnesium					
1. AZ91C-T6	-	-	11,700	16,000	
+ 5,400 ± 2,030 psi					8,200
+ 5,400 ± 4,060 psi					6,700
+ 8,100 ± 2,030 psi					9,800

TABLE VI (contd.)

Item	Thickness (inches)	K_c* (psi $\sqrt{in}$)	K_{Ic}** (psi $\sqrt{in}$)	K_{Ic}*** (psi $\sqrt{in}$)	K**** (psi $\sqrt{in}$)
2. HK31A-H24	0.160	39,800	17,300	23,000	
+ 5,400 ± 2,030 psi					13,900
+ 5,400 ± 4,060 psi					14,300
+ 8,100 ± 2,030 psi					20,500
II. Effect of Thickness					
A. Aluminum					
1. 6061-T6 (extruded)	0.160	-	15,700	21,000	
+ 8,000 ± 3,000 psi					18,800
+ 8,000 ± 6,000 psi					23,200
+12,000 ± 3,000 psi					26,600
2. 6061-T6 (extruded)	0.080	-	24,000	31,000	
+ 8,000 ± 3,000 psi					18,100
+ 8,000 ± 6,000 psi					25,100
3. 6061-T6 (extruded)	0.325	-	26,600	35,000	
+ 8,000 ± 3,000 psi					18,800
+ 8,000 ± 6,000 psi					22,300
B. Steel					
1. 4340 (150 ksi)	0.125	-	134,000	175,000	
+23,100 ± 8,700 psi					59,600
+23,100 ±17,400 psi					69,900

TABLE VI (contd.)

Item	Thickness (inches)	K_c* (psi $\sqrt{in}$)	K_{Ic}** (psi $\sqrt{in}$)	K_{Ic}*** (psi $\sqrt{in}$)	K**** (psi $\sqrt{in}$)
2. 4340 (150 ksi)	0.090	-	127,000	165,000	
+23,100 ± 8,700 psi					51,600
+23,100 ±17,400 psi					65,300
C. Titanium					
1. 6Al-4V	0.045	150,000	37,100	49,000	
+13,400 ± 5,000 psi					30,900
+13,400 ±10,000 psi					33,100
2. 6Al-4V	0.063	174,000	35,000	47,000	
+13,400 ± 5,000 psi					32,700
+13,400 ±10,000 psi					39,100
III. Effect of Cold Working					
A. Aluminum					
1. 6061-T6 (extruded) (230 shot, $6A_2$ intensity)	0.160	-	19,800	27,000	
+ 8,000 ± 3,000 psi					16,800
+ 8,000 ± 6,000 psi					23,700
+12,000 ± 3,000 psi					26,500

TABLE VI (contd.)

Item	Thickness (inches)	K_c* (psi $\sqrt{in}$)	K_{Ic}** (psi $\sqrt{in}$)	K_{Ic}*** (psi $\sqrt{in}$)	K**** (psi $\sqrt{in}$)
2. 6061-T6 (extruded) (550 shot, $15A_2$ intensity)	0.160	-	18,900	26,000	
+ 8,000 ± 3,000 psi					18,600
+ 8,000 ± 6,000 psi					23,200
+12,000 ± 3,000 psi					25,900
B. Steel					
1. 4340 (150 ksi) (110 shot, $5A_2$ intensity)	0.063	-	114,000	155,000	
+23,100 ± 8,700 psi					54,000
+23,100 ±17,400 psi					59,000
+34,500 ± 8,700 psi					76,100
2. 4340 (150 ksi) (330 shot, $7A_2$ intensity)	0.063	-	124,000	166,000	
+23,100 ± 8,700 psi					55,500
+23,100 ±17,400 psi					63,600
+34,500 ± 8,700 psi					78,700

TABLE VI (contd.)

Item	Thickness (inches)	K_c* (psi $\sqrt{in}$)	K_{Ic}** (psi $\sqrt{in}$)	K_{Ic}*** (psi $\sqrt{in}$)	K**** (psi $\sqrt{in}$)
IV. Metallurgical Effects					
A. Aluminum					
1. 6061-T4	0.160	-	13,500	18,000	
+ 8,000 ± 3,000 psi					21,700
+ 8,000 ± 6,000 psi					25,400
+12,000 ± 3,000 psi					23,100
2. 7075-T4	0.160	-	31,300	41,000	
+ 8,000 ± 3,000 psi					19,500
+ 8,000 ± 6,000 psi					22,800
+12,000 ± 3,000 psi					27,100
B. Steel					
1. 4340 (125 ksi)	0.063		107,000	146,000	
+23,100 ± 8,700 psi					58,500
+23,100 ±17,400 psi					62,900
+34,500 ± 8,700 psi					80,600

TABLE VI (contd.)

	Item	Thickness (inches)	K_c* (psi $\sqrt{in}$)	K_{Ic}** (psi $\sqrt{in}$)	K_{Ic}*** (psi $\sqrt{in}$)	K**** (psi $\sqrt{in}$)
2.	4340 (200 ksi)	0.063	153,900	110,000	147,000	
	+23,100 ± 8,700 psi					48,400
	+23,100 ±17,400 psi					53,100
	+34,500 ± 8,700 psi					66,000
V.	Effect of Chemicals					
1.	---					
2.	2024-T3 (chem-milled)	0.160	-	24,300	32,000	
	+ 8,000 ± 3,000 psi					17,900
	+ 8,000 ± 6,000 psi					23,500
	+12,000 ± 3,000 psi					24,500

*Calculated from static test data
**Calculated by equation 1, page 47
***Calculated by equation 2, page 47
****Calculated at point of failure of fatigue specimen

For fracture toughness testing the most commonly used mathematical model is that proposed by Irwin, and discussed in detail in Reference 3. The plane stress form of this equation is

$$\frac{K_c^2}{\sigma_g^2 \pi a} = \alpha_1^2 \quad \text{(Equation 1)}$$

where $\alpha_1^2 = \frac{b}{\pi a} \tan \frac{(\pi a)}{b}$ is a geometric term.

There is an indication in the literature, and in the limits of crack length imposed in Reference 3, that this mathematical model may not be the best representation for long cracks relative to specimen width. However, because of the wide general acceptance of this equation, it was decided to use it and then to convert values of stress intensity factor from fracture toughness tests to the mathematical representation used in fatigue crack propagation for comparison of static failure results from the two types of tests.

The geometric correction factor used in fatigue crack propagation is derived from the basic stress intensity equation

$$\frac{K_c^2}{\sigma_g^2 \pi a} = \alpha_2^2 \quad \text{(Equation 2)}$$

where $\alpha_2^2 = \frac{4 + 2 (a/b)^4}{[2 - (a/b)^2 - (a/b)^4]^2}$ is a geometric term.

A comparison of geometric correction factor values obtained from these two formulae for various crack lengths is shown in Figure 18. This same figure may be used to obtain the numerical relation (adjustment) between the two geometric correction factors of individual fracture toughness specimens, to calculate fatigue stress intensity factors.

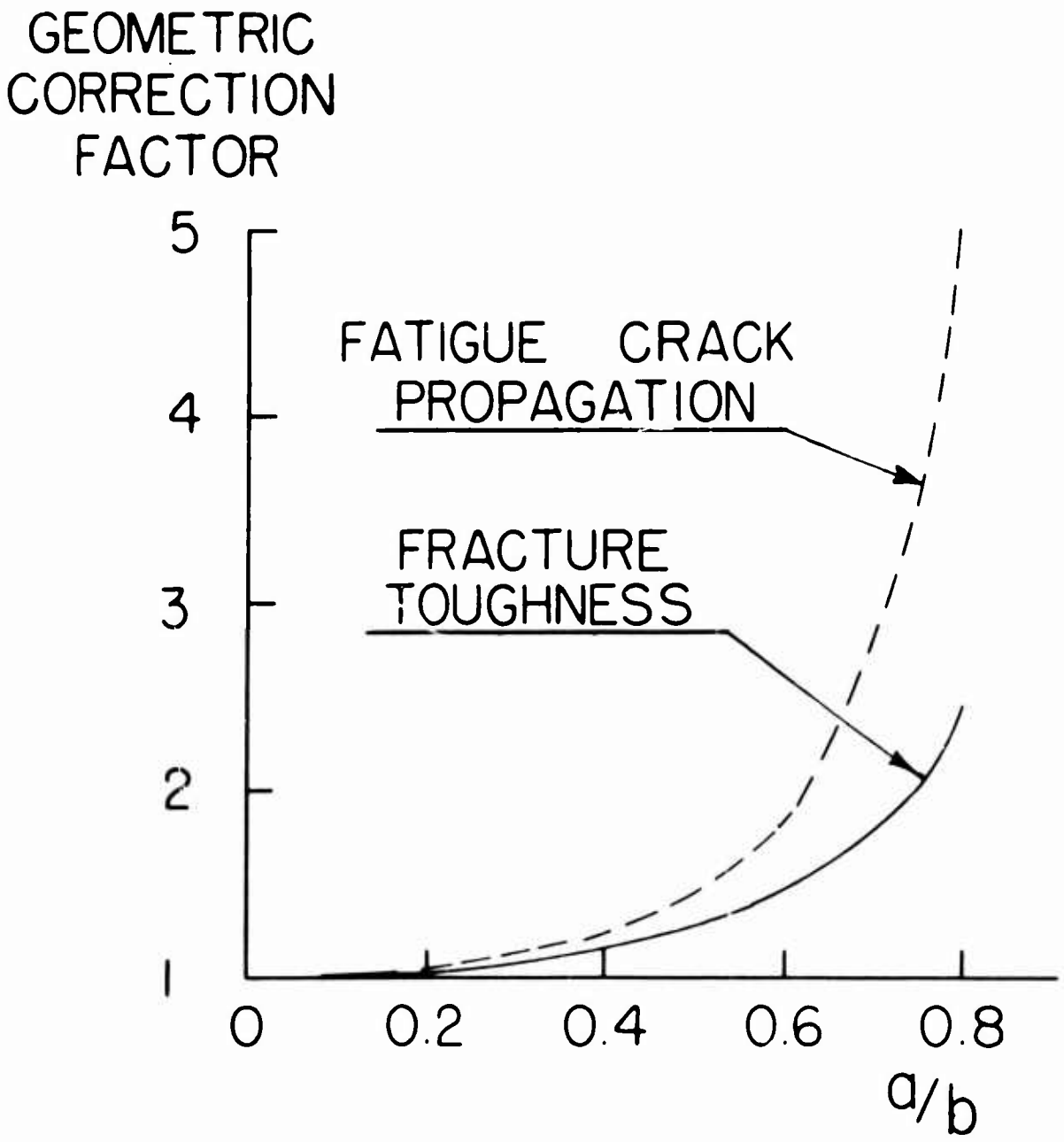

Figure 18. Comparison of Irwin and Greenspan Correction Factors

Tensile Tests

Tensile test results are tabulated in Table VII. These results are the average of the tests of each material or configuration. The values in Table VII were used in the fracture toughness tests to determine if the calculation of the stress intensity factor at failure were valid (i.e., no general yield).

All tensile test results were within the specification requirements for the materials tested, when such requirements existed.

TABLE VII

TENSILE TEST RESULTS

Item	No. of Specimens	Thickness (inches)	F_{ty} (psi)	F_{tu} (psi)	e (%)
I. Ranking of Materials					
A. Aluminum					
1. 6061-T6 (sheet)	5	0.160	40,625	44,269	12.3
2. (a) 2024-T3	5	0.160	49,869	69,682	17.6
(b) 2024-T4	6	0.160	44,183	66,700	20.5
(c) 2024-T6	5	0.160	49,876	67,660	18.0
3. 7075-T6	5	0.160	65,580	75,500	11.8
4. 7075-T6	5	0.160	78,979	84,108	9.7
5. 7001-T75	4	0.160	67,550	78,225	8.1
B. Steel					
1. 4130 (150 ksi)	6	0.063	156,054	167,403	6.4
2. 4340 (150 ksi)	6	0.063	138,346	150,566	9.0
3. 301 (1/4 hard)	6	0.063	102,858	146,478	30.4
4. 410 (cond. "T")	6	0.063	119,152	135,392	7.8
5. 18% Ni Maraging Steel (250 Grade)	5	0.063	263,659	268,667	2.6
C. Titanium					
1. Ti 140A	6	0.090	117,504	133,405	16.8
2. Commercially Pure	6	0.090	66,227	85,530	22.7
3. 8Al-1Mo-1V (Duplex annealed)	5	0.090	137,749	148,949	12.3
4. 6Al-4V (annealed)	6	0.090	140,473	147,826	14.3
5. 5Al-2.5Sn (annealed)	5	0.063	130,316	137,939	13.8

TABLE VII (contd.)

Item	No. of Specimens	Thickness (inches)	F_{ty} (psi)	F_{tu} (psi)	e (%)
D. Magnesium					
1. AZ91C-T6	5	0.300	12,535	24,395	2.9
2. HK31[illegible]-H24	5	0.160	30,500	36,500	9.1
E. Laminated Plastics					
1. (a) 181 glass cloth (warp)	5	0.170	-	52,068	-
(b) 181 glass cloth (fill)	5	0.170	-	47,088	-
(c) 181 glass cloth (45°)	5	0.170	-	27,325	-
2. (a) 143 glass cloth (warp)	5	0.170	-	81,666	-
(b) 143 glass cloth (fill)	5	0.170	-	7,447	-
(c) 143 glass cloth (45°)	5	0.170	-	12,840	-
II. Effect of Thickness					
A. Aluminum					
1. 6061-T6 (extruded)	5	0.160	37,620	44,847	14.2
2. 6061-T6 (extruded)	6	0.080	37,064	42,652	12.5
3. 6061-T6 (extruded)	6	0.325	44,900	50,016	18.2
B. Steel					
1. 4340 (150 ksi)	7	0.125	164,537	176,489	8.8
2. 4340 (150 ksi)	5	0.090	156,180	167,580	9.6
C. Titanium					
1. 6Al-4V (annealed)	6	0.045	141,173	149,989	7.8
2. 6Al-4V (annealed)	6	0.063	140,394	147,020	11.3

TABLE VII (contd.)

Item	No. of Specimens	Thickness (inches)	F_{ty} (psi)	F (psi)	e (%)
III. Effect of Cold Working					
A. Aluminum					
1. 6061-T6 (extruded) (230 shot, $6A_2$ intensity)	6	0.160	39,600	46,317	11.0
2. 6061-T6 (extruded) (550 shot, $15A_2$ intensity)	6	0.160	43,489	50,658	11.0
B. Steel					
1. 4340 (150 ksi) (110 shot, $5A_2$ intensity)	6	0.063	151,181	166,127	7.8
2. 4340 (150 ksi) (330 shot, $7A_2$ intensity)	6	0.063	137,262	157,260	8.7
IV. Metallurgical Effects					
A. Aluminum					
1. 6061-T4 (sheet)	6	0.160	19,316	36,583	26.4
2. 7075-T4	6	0.160	46,487	71,517	17.4

TABLE VII (contd.)

Item	No. of Specimens	Thickness (inches)	F_{ty} (psi)	F_{tu} (psi)	e (%)
B. Steel					
1. 4340 (125 ksi)	6	0.063	124,346	136,307	12.3
2. 4340 (200 ksi)	5	0.063	198,225	214,006	4.6
V. Effect of Chemicals					
A. Aluminum					
1. 6061-T6 (extruded)	5	0.160	37,620	44,847	14.2
2. 2024-T3 (chem-milled)	6	0.160	51,759	67,934	18.2
B. Steel					
1. 4340 (150 ksi, UTS)	5	0.063	138,346	150,566	9.0

CONCLUSIONS

It is concluded that:

1. The materials considered in this research program have been ranked for their resistance to fatigue crack propagation at steady and vibratory stresses representative of service fatigue environments.

2. A statistically reliable basis of fatigue crack propagation data has been obtained for further analysis and research.

3. Two fatigue crack propagation retardants have been evaluated: (a) dodecyl alcohol film, considered unsuccessful; (b) shot-peening, considered successful and worth further research and application.

4. For the materials tested, the correlation between fracture toughness and the last stages of fatigue crack propagation (static fracture) is very poor. It is further concluded that the application of fracture toughness parameters to fatigue crack propagation final static failure would lead to small, non-conservative errors in cracked life estimates.

5. A general trend has been observed in resistance to fatigue crack propagation; ductile, lower-ultimate-strength materials show greater resistance to fatigue crack propagation. With dependable field inspection techniques for very small fatigue cracks, the designer of a structure should consider lower fatigue initiation strength materials, coupled with inspection aids and a long fatigue-cracked life, to achieve an over-all higher reliability than can be gained by dependence on structural strength alone.

6. Since fracture toughness equations were derived for homogeneous, isotropic media, the application of fracture toughness parameters to plastic laminates is not within the state of the art.

7. Plastic laminate fatigue crack propagation results have a strong dependence on the prior stress history of the laminate.

RECOMMENDATIONS

It is recommended that research be continued into the theory of basic mechanisms of fatigue crack propagation. This further research should include the following areas:

1. Attempt to rationalize the differences in fracture toughness parameters obtained from static and fatigue crack propagation tests, particularly evaluating secondary stress intensity factors indicated by Muskhelishvili's basic studies, Reference 7.

2. Determine if there is, in fact, any mathematical relationship between fatigue crack propagation and fracture toughness parameters.

3. Determine a mathematical relationship governing the effect of steady and vibratory stresses on fatigue crack propagation.

4. Evaluate fatigue crack propagation initiated by ballistic penetration.

5. Evaluate the effects of compressive stress fatigue crack retardants (especially shot-peening) as a function of the applied stress and the profile of residual compressive stresses and as a function of the ratio of the compressive layer thickness to the specimen thickness.

6. Determine if, in fact, the effect of compressive stress fatigue crack retardants diminishes by the effect termed cyclic induced stress relaxation.

7. Continue accumulation of fatigue crack propagation information as a routine analysis of new engineering materials.

8. Continue basic studies of composite materials to develop mathematical techniques necessary to analyze and categorize fatigue crack propagation data in these materials.

9. Develop methods to promote fracture toughness study from its present level as an academic interest area for the fracture mechanics physicist to a useful technology for the designer and structures engineer.

BIBLIOGRAPHY

1. Boyle, R., "A Method for Determining Crack Growth", Materials Research and Standards, Volume 2, No. 8, August 1962, pp. 646-651.

2. Christensen, R., "Fatigue-Crack Growth Affected by Metal Fragments Wedged Between Opening-Closing Crack Surfaces", Douglas Aircraft Independent Research Program Account No. 81296-154, Sept. 1962.

3. Fracture Toughness Testing and Its Applications, ASTM Special Technical Publication No. 381, American Society for Testing and Materials, Philadelphia, Pa., 1965.

4. Frankel, H., Bennett, J., Holshauser, W., "Effect of Oleophobic Films on Metal Fatigue", Journal of Research of the National Bureau of Standards, Volume 64C, No. 2, April-June 1960.

5. Greenspan, M., "Axial Rigidity of Perforated Structural Members", Journal of Research of the National Bureau of Standards, Volume 31, Dec. 1943, pp. 305-322.

6. Metal Improvement Company, Doctor H. O. Fuchs, Consultant, Private Consultation.

7. Muskhelishvili, N., Some Basic Problems of the Mathematical Theory of Elasticity, P. Noordhoff Ltd., Groningen-The Netherlands, 1963.

DISTRIBUTION

US Army Materiel Command	5
US Army Mobility Command	5
US Army Aviation Materiel Command	6
US Army Aviation Materiel Laboratories	29
US Army Engineer R&D Laboratories	2
US Army Research Office-Durham	1
Plastics Technical Evaluation Center	1
US Army Engineer Waterways Experiment Station	1
US Army Quartermaster School	2
US Army Infantry Center	2
US Army Tank-Automotive Center	2
US Army Aviation Maintenance Center	2
US Army Armor and Engineer Board	1
US Army Electronics Command	2
US Army Aviation Test Activity	2
Air Force Flight Test Center, Edwards AFB	2
US Army Field Office, AFSC, Andrews AFB	1
Air Force Systems Command, Wright-Patterson AFB	1
Air Force Flight Dynamics Laboratory, Wright-Patterson AFB	1
Systems Engineering Group (RTD), Wright-Patterson AFB	3
Bureau of Naval Weapons, DN	6
Office of Naval Research	1
Chief of Naval Research	2
US Naval Research Laboratory	1
David Taylor Model Basin	1
Commandant of the Marine Corps	1
Ames Research Center, NASA	1
Lewis Research Center, NASA	1
Manned Spacecraft Center, NASA	1
NASA Representative, Scientific and Technical Information Facility	2
Research Analysis Corporation	1
NAFEC Library (FAA)	2
Aeronautical Materials Laboratory	1
Defense Documentation Center	20

APPENDIX

MATERIALS

Materials tested in this program were purchased under standard military specifications applied to engineering materials used in the aerospace industry. The list of materials tested is given below.

I. Ranking of Materials	Specification
A. Aluminum	
1. 6061-T6 sheet	QQ-A-327
2. 2024-T3 sheet Processed in accordance with MIL-H-6088C to T4 and T6	QQ-A-362
3. 7075-T6 sheet	QQ-A-287
4. 7178-T6 sheet	QQ-A-250/15
5. 7001-T75 Ti.02, Si.12, Fe.16, Cu2.26, Mn.04, Mg3.03, Cr.21, Ni.01, Zn7.61	none available - chemistry below
B. Steel	
1. 4130 Processed in accordance with MIL-H-6875B	MIL-S-18729B
2. 4340 Processed in accordance with MIL-H-6875B	AMS-6359A
3. 301, 1/4 hard	MIL-S-5059A
4. 410 cond. "T" Processed in accordance with MIL-H-6875B	QQ-S-763
5. 18% Ni Maraging Steel (250 Grade) Vanadium Alloys, Vacuum Melted, Heat 34021 C.02, S.05, Mn.03, S.005, P.002, Al.06, Ti.33, B.005, Mo4.90, Co7.82, Ni18.65, Zr.0085, Ca.02 (added)	

		Specification
C.	Titanium	
	1. Ti-140A (2Fe-2Cr-2Mo)	MIL-T-9046C Class 4
	2. Commercially Pure	MIL-T-9046C Class 7
	3. 8Al-1Mo-1V (Duplex annealed)	MIL-T-9046D Type II Composition F
	4. 6Al-4V	MIL-T-9046C Class 2
	5. 5Al-2.5Sn	MIL-T-9046C Class 3
D.	Magnesium	
	1. AZ91C-T6 Processed by vendor (Wellman Bronze) in accordance with	QQ-M-56 MIL-M-6875B
	2. HK31A-H24	AMS-4385
E.	Laminated Plastics	
	1. 181/150 glass cloth	
	(a) cloth specification	MIL-C-9084B Type VIII A
	(b) finish	Volan A
	(c) resin specification	MIL-R-9300A
	(d) vendor (resin) (E-293) Cordo Division of Ferro Corp.	
	(e) resin content	38%
	(f) other variables Cure Temp. 340°F, Cure Time 2 hrs., Press. 50 psig 25" Hg vacuum	
	2. 143 glass cloth	
	(a) cloth specification	MIL-C-9084B Type V
	(b) finish	Volan A
	(c) resin specification	MIL-R-9300A

		Specification
(d)	vendor (resin) (E-293) Cordo Division of Ferro Corp.	
(e)	resin content	41.8%
(f)	other variables Specific Gravity	1.75
	Cure Temp. 340°F, Cure Time 2 hrs., Press. 50 psig 25" Hg vacuum	

II. Effect of Thickness

A. Aluminum

1. 6061-T6 (extruded) Processed in accordance with except that solution heat-treatment temperature range was 910°- 930°F — QQ-A-270A MIL-H-6088C

B. Steel

1. 4340 (150 ksi) 0.090" Processed in accordance with (Rockwell C36 hardness) — AMS-6359A MIL-H-6875B

2. 4340 (150 ksi) 0.125" Processed in accordance with (Rockwell C36 hardness) — AMS-6359A MIL-H-6875B

III. Effect of Cold-Working

A. Aluminum

NOTE: All specimens were peened by Metal Improvement Company, Hackensack, N. J. using a Gantry unit; specimen feed rate - 6 inches per minute, oscillation - 20 strokes per minute.

1. 6061-T6 230 shot, 6A2 measured intensity

2. 6061-T6 550 shot, 15A2 measured intensity

B. Steel — Specification

1. 4340 (150 ksi) 110 shot, 5A2 intensity

2. 4340 (150 ksi) 330 shot, 7A2 intensity

IV. Metallurgical Effects

A. Aluminum

1. 6061-T4 processed in accordance with MIL-H-6088C

2. 7075-T4 processed in accordance with MIL-H-6088C to 7075-W Room temperature age for minimum of 96 hours to -T4 condition

B. Steel

1. 4340 (125 ksi) processed in accordance with MIL-H-6875B

2. 4340 (200 ksi) processed in accordance with MIL-H-6875B

V. Effect of Chemicals

A. Aluminum

1. Defined above

2. 2024-T3 chem-milled; chemically milled in a proprietary solution — QQ-A-355 (T3)

Sodium hydroxide buffered with sodium sulphide and sodium gluconate.

Unclassified
Security Classification

DOCUMENT CONTROL DATA - R&D

(Security classification of title, body of abstract and indexing annotation must be entered when the overall report is classified)

1. ORIGINATING ACTIVITY (Corporate author)	2a. REPORT SECURITY CLASSIFICATION
Sikorsky Aircraft Division of United Aircraft Corporation	Unclassified
	2b. GROUP

3. REPORT TITLE

FATIGUE CRACK PROPAGATION IN AIRCRAFT MATERIALS

4. DESCRIPTIVE NOTES (Type of report and inclusive dates)

Test Data - February 25, 1963 to August 31, 1965

5. AUTHOR(S) (Last name, first name, initial)

Degnan, William G., Dripchak, Peter D., Matusovich, Charles J.

6. REPORT DATE	7a. TOTAL NO. OF PAGES	7b. NO. OF REFS
March 1966	61	Six

8a. CONTRACT OR GRANT NO.	9a. ORIGINATOR'S REPORT NUMBER(S)
DA 44-177-AMC-84(T)	USAAVLABS Technical Report 66-9
b. PROJECT NO. Task 1P125901A14227	
c.	9b. OTHER REPORT NO(S) (Any other numbers that may be assigned this report)
d.	SER-50411

10. AVAILABILITY/LIMITATION NOTICES

Distribution of this document is unlimited.

11. SUPPLEMENTARY NOTES	12. SPONSORING MILITARY ACTIVITY
	US Army Aviation Materiel Laboratories Fort Eustis, Virginia

13. ABSTRACT The influence of metallurgical, chemical, and geometric variables on fatigue crack propagation rates were investigated in alloys of aluminum, magnesium, steel, and titanium. Some limited fatigue crack propagation was done in laminated plastics. A possible correlation between fatigue crack propagation, fracture toughness, and tensile strength was also investigated.

All materials have been ranked according to their resistance to fatigue crack propagation. The critical plane strain fracture toughness (K_{Ic}), critical plane stress fracture toughness (K_c) (where applicable), ultimate tensile strength, and per cent elongation were also reported for all materials.

For the materials tested in this program there was no appreciable thickness or chemical effect. Shot-peening did increase resistance to fatigue crack propagation. In general there was an increase in the resistance to fatigue crack propagation in materials with greater ductility. The correlation between fatigue crack propagation and static fracture toughness was very poor. The crack propagation results of laminated plastics was also considered unsatisfactory.

Further research is needed to determine the effect of steady and vibratory stresses on fatigue crack propagation. Research is needed to determine the relationship between fatigue crack propagation and fracture toughness parameters.

DD FORM 1 JAN 64 1473

Unclassified
Security Classification